

## EFFECT OF STIR CASTING PROCESS PARAMETERS AND STIRRER BLADE GEOMETRY ON MECHANICAL PROPERTIES OF Al MMCS – A REVIEW

Aluminium matrix composites offer a combination of properties such as lower weight, higher strength, higher wear resistance and many more. The stir casting process is easy to use, involves low cost and is suitable for mass production compared to other manufacturing processes. An in-depth look at recently manufactured aluminium matrix composites and their impact on particle distribution, porosity, wettability, microstructure and mechanical properties of Al matrix composites have all been studied in relation to stirring parameters. Several significant concerns have been raised about the sample's poor wettability, porosity and particle distribution. Mechanical, thermal, and tribological properties are frequently studied in conjunction with variations in reinforcement proportion but few studies on the effect of stirrer blade design and parameters such as stirrer shape, dimensions and position have been reported. To study the effect of stirrer blade design on particle distribution, computational fluid dynamics is used by researchers. Reported multiphysics models were  $k-\varepsilon$  model and the  $k-\omega$  model for simulation. It is necessary to analyse these models to determine which one best solves the real-time problem. Stirrer design selection and analysis of its effect on particle distribution using simulation, while taking underlying physics into account, can be well-thought-out as a future area of research in the widely adopted stir casting field.

*Keywords:* Metal matrix composites (MMCs); Aluminium; Mechanical properties; Particle distribution; Stirrer design

### 1. Introduction

Recent advancements in technology and constant need of improvement in product quality requires focus on the development of novel materials. Materials can be considered as the backbone in the current era of industries. The possibility of mixing different materials such as metal and their alloys, polymers and ceramics provide the opportunity for obtaining varieties of functional properties (Fig. 1). A composite material is a combination of distinct materials having unique chemical and physical properties in which aim is to gain favourable properties of distinct materials. So, very detailed knowledge is required about the materials to select suitable materials for fabrication of composites [1,2]. Natural composites are available in animals and plants. Examples are wood, teeth, bone and abalone shell. In market, composite materials are gaining attraction due to the advantage of obtaining combination of properties that cannot be attained otherwise [3]. Metal do not always have necessary characteristics required for all working conditions. To achieve required properties for specific condition, one possible way is to

reinforce those alloys with certain amount of ceramic particles. Materials fabricated by reinforcing ceramic particles with base alloy are known as metal matrix composites (MMCs). The matrix material is a soft metallic material having certain mechanical and physical properties. The material that is added in the

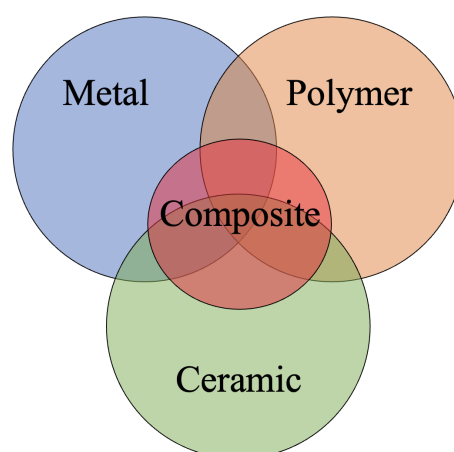


Fig. 1. Family of composite materials

<sup>1</sup> SARDAR VALLABHBHAI NATIONAL INSTITUTE OF TECHNOLOGY, DEPARTMENT OF MECHANICAL ENGINEERING, SURAT, GUJARAT, INDIA

<sup>2</sup> RESEARCH SCHOLAR, DEPARTMENT OF MECHANICAL ENGINEERING, SARDAR VALLABHBHAI NATIONAL INSTITUTE OF TECHNOLOGY, ICHCHHANATH, SURAT, 395007, GUJARAT, INDIA

\* Corresponding author: [cmmail9003@gmail.com](mailto:cmmail9003@gmail.com)



matrix material which provides good bonding and strengthens matrix material is known as reinforcement. Selection of matrix material and reinforcement material depends on the required mechanical properties such as hardness, tensile strength, wear resistance, cost advantage and availability in the market. Now a days, MMCs are used in the field of aerospace, automobile, defense, marine and general engineering applications due to its light weight, higher strength to weight ratio, corrosion resistance, wear resistance, enhanced high temperature performance, improved creep and fatigue resistance and many more combination of properties [4].

Selvam et al., [1] reviewed different matrix materials such as Aluminium (Al), Copper (Cu), Magnesium (Mg) and discussed in detail about various reinforcement particles used to obtain required properties. They also reviewed various methods to improve wettability such as adding wettability agents and fluxes, preheating ceramic particle and coating the ceramic particles. But these processes led to the increment in manufacturing costs. They also concluded that better properties can only be attained if reinforcements are distributed uniformly and not agglomerated in the matrix. The provided comprehensive review of reinforcement materials facilitates the selection of reinforcement materials that are suitable for the intended uses. There are other additional criteria also that must be considered during the production of MMCs. Muhammad & Jalal [5] provided comparative study on the impact of stirrer design parameters on quality of fabricated MMCs. Major important parameters reported were number of blades, stirrer geometry, blade angle, impeller diameter and position. Flow pattern during stirring cannot be observed due to closed non transparent furnace, hence direct visualization is not possible and effective. To overcome these problems, they reported statistical analysis and numerical simulation besides experiments. They also mentioned that stirrer design and speed together affect flow behaviour and it is difficult to differentiate between two. Number of stirrer stages also affects homogenous particle distribution. Temperature, viscosity and density of melt, type of stirrer, shape of impeller and state of mixed phases affects mixing capability. Due to complexity and large number of variables affecting stirrer design, researchers were not able to generalize their findings. This article offers a more in-depth examination of the factors affecting stir cast MMCs. For the selection of stirrer shape and dimensions, a comprehensive analysis of existing stirrer blade design and its effect on the qualities of manufactured MMCs will be more beneficial. Samal et al., [6] reported future work in developing the methods to reduce porosity in the composites and improving wettability of the composite for better bonding between matrix and reinforcements. They suggested to study the effect of biofiber and industrial waste in hybrid MMCs for the improvement in strengthening mechanism. They also mentioned to study formation of nano composites and suggested to apply mathematical modelling techniques in prediction of wear and mechanical properties. In the field of stir cast MMCs, two additional factors, such as hybrid reinforcement and nano reinforcement, are addressed in this review. With nano reinforcement, however, the issue of wettability requires greater attention.

Zhou et al., [7] focused on reviewing progress in hybrid reinforcements, fabrication methods, properties and strengthening mechanisms. The hybrid reinforcements were categorized into hybrid continuous and discontinuous reinforcements, hybrid micron discontinuous reinforcements, hybrid nano discontinuous reinforcements and hybrid multi scale discontinuous reinforcements. Hybrid reinforcements were realized to be useful in automobile and aerospace industries due to possibility of achieving tougher, lighter and stronger materials. To attain required properties of hybrid reinforced MMCs, the key parameters reported were homogeneous distribution of particles, good interfacial bonding between matrix and reinforcements and structural integrity of reinforcements. Ramanathan et al., [8] provided detailed review and opportunities in the field of MMCs. They reviewed stir casting furnace designs in detail. They also suggested opportunities to study certain parameters such as reduction in porosity, the effect of various stirrer blade profiles for uniform distribution of reinforcement particles, wettability improvement of reinforcement with matrix and finding recycling techniques for both matrix and reinforcements. This article includes an in-depth examination of the stir casting process and its parameters, although one of the factors, stirrer blade design and dimensions, need additional attention for the development of MMC characteristics. Garg et al., [9] reported that nano size particles are difficult to synthesize using conventional stir casting because of poor distribution of particles inside the melt and result into high porosity. It was observed that wettability of particles inside matrix melt decreases with increase in weight percent of particle reinforcement and decrease in particle size. They discussed briefly about commercialization of Al MMCs. Major concern was related to cost / performance ratio. It is expected that Al MMCs may be used for large scale production in future to come. They focused on nanoparticle reinforcement and its associated drawbacks. In addition to examining the influence of reinforcement variation on the properties of manufacturable MMCs, the research in the direction of the commercialization of MMCs should receive more attention.

Sahu & Sahu [10] reviewed Al MMCs fabrication and stirring process parameters optimization. They considered stirring process parameters important for understanding distribution of reinforcements. Some of significant parameters mentioned were stirring speed, blade angle, stirring time, stirrer size, stirrer position and feed rate of reinforcements. Stirrer design needs to be such that it minimizes power requirement and provide high degree of axial flow. Researcher used water based model and computational fluid dynamics (CFD) model to study effect of impeller blade angle on particle distribution. They also suggested the relation between impeller diameter ( $d$ ), crucible diameter ( $D$ ) and blade width ( $b$ ). The recommended impeller diameter for crucibles with flat bases was 0.5 times that diameter, whereas for crucibles with semi-spherical bases, it was 0.55 times that diameter. The blade's breadth should be between 0.1 and 0.2 times the crucible's diameter. Optimal feeding rate of reinforcement reported was 0.8 to 1.5 g/s to avoid clustering and achieve homogeneous distribution. This review aided in the

selection of stirrer dimensions, however the selection of stirrer shape is a significant difficulty and the selection of dimensions will vary based on shape. Detailed research on the optimal shape and size of stirrer blades in consideration of other parameters is necessary. Razzaq et al., [11] reviewed in detail about wettability improvement between Al matrix and reinforcement materials. Wettability improvement does not only refer to the governing of contact angle but strategies involved to improve dispersion, engulfment and distribution of particles in metal matrix are also called wettability. They reported different studies for improvement of wettability between matrix and reinforcements such as addition of wetting agents, fluxes, preheating the reinforcement particles, coating the reinforcement particles and using composting techniques. They mentioned that reactive elements such as Li, Mg, Ca, Ti, Zr and P promotes the wettability between metal and reinforcement at the interface by inducing chemical reaction. They suggested two basic methods to improve wettability. The first is surface modification of reinforcement material and the second is melting treatment technique. Homogeneous particle distribution is affected by stirring parameters such as stirrer shape, stirrer dimension, stirrer position and stirring time [12]. Selection of stirrer material and its design is also important to optimize the cost. Selected materials must have sufficient mechanical strength, chemical stability to avoid any contamination. It should be heat resistant and easily machinable [13].

Almost all the available review papers were focused on matrix material, reinforcement material, MMC manufacturing processes and stir casting parameters. From reviewed papers, list of mostly used reinforcement materials and their properties is provided to make reinforcement selection process easy for focused applications. Lack of discussion is observed concerning effect of stirrer blade design on properties and microstructure of

MMCs. This paper presents a summary of widely used matrix materials, reinforcement materials, and MMC production techniques. Next, a comprehensive overview of recent articles on stir casting process and the influence of its parameters on the characteristics of Al MMCs is presented. This review focuses primarily on the influence of stirrer blade design and its parameters on the characteristics of MMCs. Finally, Al MMCs applications are recommended along with potential future developments in the stir casting field.

## 2. Matrix and Reinforcement Materials

### 2.1. Matrix Materials

Metal matrix composites are having at least two constituents, one having metallic materials such as Al, Mg, Cu, Titanium (Ti), Silver (Si), Nickel (Ni) and intermetallics, other being metal or any other material such as ceramic or organic materials. According to the needs, the properties of these matrix materials can be changed by adding different reinforcement elements [14]. If more than two reinforcement materials are present in MMC than it is called hybrid metal matrix composites. Mostly reported matrix and reinforcement materials used for production of MMCs are listed in Fig. 2.

Copper MMCs are useful in many engineering applications where better microstructural stability and high temperature is required. Cu MMCs are an effective choice as friction material for heavy-loaded, high-speed applications, such as high-speed trains and airplanes, as they readily dissipate the heat generated [15,16]. Magnesium MMCs provide suitable properties for automobile and aerospace components such as good mechanical

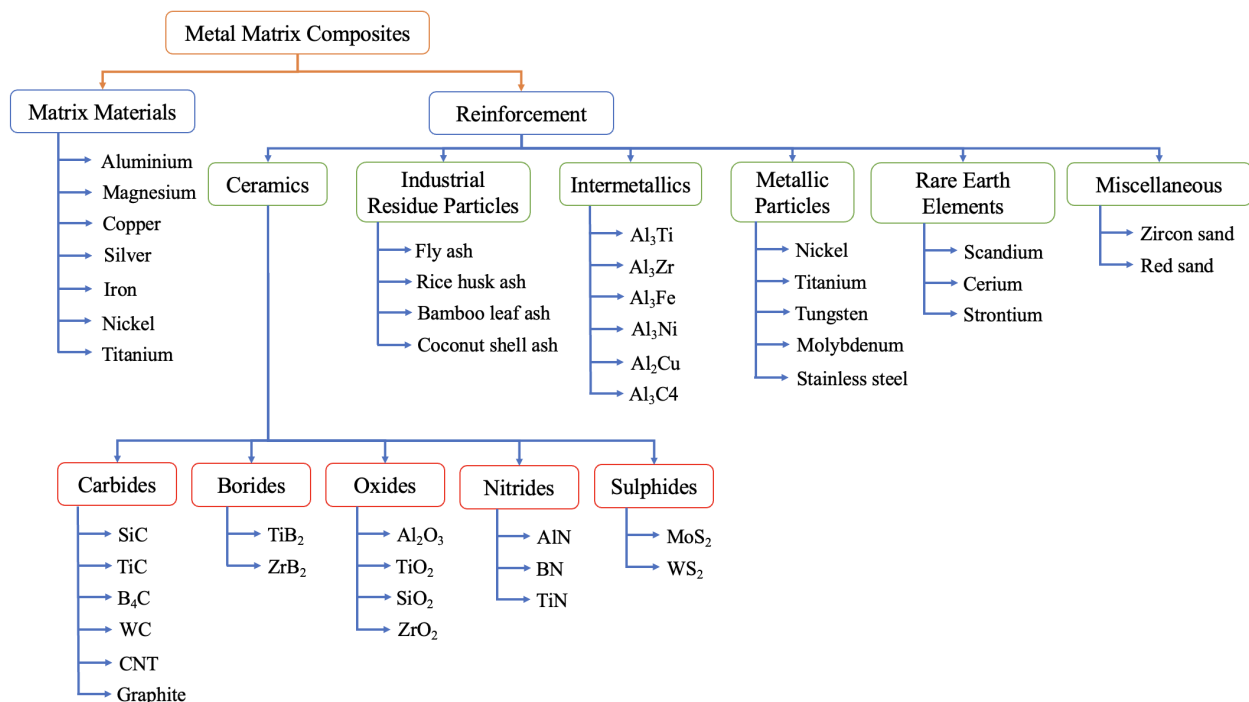


Fig. 2. Matrix and reinforcement materials used for production of MMCs

properties, low density, higher corrosion resistance and wear resistance. They also have low thermal coefficient of expansion as compared to other metal and alloys. However, their ductility was reduced which limits their applications. Magnesium alloys are also used where light weight is of main importance [17,18]. Titanium MMCs are mostly prepared to improve insufficient elastic modulus, hardness and wear resistance of Ti alloy. Ti MMCs offer high stiffness and specific strength compared to steel and nickel base materials. High temperature Ti MMCs also provide 50% weight reduction compared to monolithic alloys [19]. TiB and TiC are the suitable and effective reinforcements among the several reinforcement materials due to high reactivity of titanium at elevated temperature. Main drawback is reinforcing Ti with strong ceramic phase lead to poor ductility which limits its application in various fields [20]. Nickel alloys exhibit excellent mechanical and tribological properties at elevated temperatures which expands its applications in marine, aerospace and turbine engines but high density and poor creep resistance limits its application. Nickel MMCs were prepared to overcome these problems by reinforcing suitable ceramic materials. Reinforcements such as Gr, SiO<sub>2</sub>, Al<sub>2</sub>O<sub>3</sub> and Carbon Nano Tube (CNT) are used to improve mechanical properties. Development of novel and cost effective manufacturing method for Ni MMCs is also very important [21,22]. As the matrix material, various steels and pure iron-based materials have also been used. Austenitic steel 316L is the most commonly used stainless steel (SS) due to its advantages such as good corrosion resistance and high toughness. To improve wear resistance, reinforcement materials such as Al<sub>2</sub>O<sub>3</sub>, ZrO<sub>2</sub>, SiC, TiN and TiC were used. It has also been reported that the use of WC-Co powder improves the micro hardness of the cladding layer during laser cladding [23-25]. Destructive tribological testing is required for silver and its alloys which are used in structural components. In electrical parts, development of adhesive bonds at early temperature rise leads to tribological wear. To overcome this issue, silver alloys are reinforced with ceramic particles such as SiC, glassy carbon and Al<sub>2</sub>O<sub>3</sub>. Addition of ceramic particles resulted in smaller friction coefficient values and low friction wear. Reinforcement addition may also improve hardness and mechanical properties [26]. When two dissimilar metals are combined following rules of chemical valence, intermetallics are formed. They are ionic and covalent in nature. They are brittle having complex crystal structures and sometimes used as matrix material in MMCs. Intermetallics are mainly used to improve

potential operating temperature over conventional materials. MoSi<sub>2</sub> is an important intermetallic commonly used as heating element in furnaces. It has high melting point and good stability at high temperatures in an oxidizing atmosphere [27]. Al MMCs are most widely used in market owing to low cost, low density, high strength to weight ratio, better corrosion and wear resistance and toughness. They are used in the field of defense, automotive, marine and aerospace. Researchers in Al-based MMCs are intended more to substitute materials such as Al alloy, ferrous alloys, titanium alloys and polymer-based composites in many applications. Commonly used reinforcements for preparation of Al MMCs are SiC, Al<sub>2</sub>O<sub>3</sub>, B<sub>4</sub>C, AlN, BN, graphene, CNT and residue particles such as fly ash, rice husk ash, bamboo ash and coconut shell ash [2,27].

Among all above listed materials, easy availability, light weight and low cost of Al and its alloys compared to other materials make it widely selected material by researcher in the field of MMCs. Many researches are working to improve specific properties of Al alloy by mixing it with different reinforcement materials to make it suitable in the field of automotive, aerospace, marine and defense.

## 2.2. Reinforcement materials

Reinforcement materials are mostly non-metallic materials having specific properties. Selection of reinforcement materials plays a vital role in the preparation of MMCs. To achieve the required properties of MMCs selection of suitable reinforcement material is necessary. Selection of reinforcement depends on matrix type, reinforcement shape and size, the type of processing of composites and interfacial bonding between matrix and reinforcement. Reinforcement materials are available in the form of continuous fibers, short fibers, whiskers or particles [27,28]. TABLE 1 lists key characteristics of various types of reinforcing materials as well as potential interfacial bonding mechanisms with Al.

## 3. Techniques for Manufacturing of MMCs

MMCs can be fabricated by varieties of methods. Most of the methods are divided mainly based on liquid state and solid state manufacturing [48]. Properties of MMCs such as strength,

TABLE 1

List of different types of reinforcement materials' properties and possible interfacial bonding mechanisms with Al

Sr. No.	Reinforcement	Properties	Mechanism of Interfacial Bonding with Al	References
1	SiC	<ul style="list-style-type: none"> <li>• Hardness is high</li> <li>• Thermal expansion is low</li> <li>• Thermal conductivity is high</li> <li>• Corrosion resistant and abrasion resistant</li> </ul>	<ul style="list-style-type: none"> <li>• The primary reaction of Al-SiC at the interface produces Al<sub>4</sub>C<sub>3</sub>. As Al<sub>4</sub>C<sub>3</sub> is insoluble and brittle in nature, it forms as a separate precipitate or as a continuous layer around the SiC particles.</li> <li>• The Al<sub>4</sub>C<sub>3</sub> layer at the interface increases ultimate tensile strength, the average yield strength, and work hardening rate while reducing the material's ductility slightly.</li> </ul>	[1,29]

TABLE 1. Continued

2	Al <sub>2</sub> O <sub>3</sub>	<ul style="list-style-type: none"> <li>• Thermal expansion coefficient is high</li> <li>• Better electrical insulation</li> <li>• Good bonding with molten Al</li> <li>• Hardness is high</li> <li>• Better working capability at high temperature</li> </ul>	<ul style="list-style-type: none"> <li>• Because Al<sub>2</sub>O<sub>3</sub> is stable in pure molten aluminium, the presence of Al aids in achieving good bonding with molten Al and produces no reaction products at the interface.</li> <li>• However, if Mg is present in the alloy, Al<sub>2</sub>O<sub>3</sub> will react with Mg. MgO is expected to form at the interface with high levels of Mg in the matrix, whereas spinel (MgAl<sub>2</sub>O<sub>4</sub>) forms at low levels of Mg.</li> </ul>	[4,27,30,31]
3	B <sub>4</sub> C	<ul style="list-style-type: none"> <li>• Hardness is high</li> <li>• Abrasion and corrosion resistant</li> <li>• Density is low</li> <li>• Chemically inert</li> <li>• Melting point is high</li> <li>• Thermally stable at elevated temperature</li> </ul>	<ul style="list-style-type: none"> <li>• The reaction products of Al and B<sub>4</sub>C are AlB<sub>2</sub>, Al<sub>4</sub>BC, Al<sub>4</sub>C<sub>3</sub>, and AlB<sub>24</sub>C<sub>4</sub> depending on the temperature.</li> <li>• The formation of Al<sub>4</sub>C<sub>3</sub> would significantly reduce composite mechanical properties. Al<sub>4</sub>BC has a positive effect on hardness but has a negative effect on material fracture toughness.</li> </ul>	[1,32]
4	TiC	<ul style="list-style-type: none"> <li>• Thermal conductivity is high</li> <li>• High abrasion resistance</li> <li>• Melting point is high</li> <li>• Hardness is high</li> </ul>	<ul style="list-style-type: none"> <li>• The reaction products formed are large Al<sub>3</sub>Ti precipitates in the matrix's bulk and Al<sub>4</sub>C<sub>3</sub> blocks at the particle-matrix interface. TiC dissolution in pure Al is much slower than SiC dissolution.</li> <li>• MMC stiffness and strength are increased by the presence of Al<sub>3</sub>Ti.</li> </ul>	[1,33]
5	WC	<ul style="list-style-type: none"> <li>• Corrosion resistant</li> <li>• Electrical conductivity is good</li> <li>• Thermal conductivity is good</li> <li>• Melting point is high</li> <li>• Hardness is high</li> </ul>	<ul style="list-style-type: none"> <li>• Particle reinforced Al MMCs with WC forms WA<sub>12</sub>, WA<sub>15</sub>, and Al<sub>4</sub>C<sub>3</sub> that vary with temperature at the interface between the carbide and Al.</li> <li>• Formation of such hard intermetallics at interface improves hardness and strength of the composites.</li> </ul>	[1,34]
6	AlN	<ul style="list-style-type: none"> <li>• Dielectric constant is low</li> <li>• Stiffness is high</li> <li>• More chemically stable than SiC</li> <li>• Thermal conductivity is high</li> <li>• Electrical resistivity is high</li> </ul>	<ul style="list-style-type: none"> <li>• The presence of Al aids in achieving good bonding with molten Al and produces no reaction products at the interface.</li> </ul>	[1,4]
7	TiB <sub>2</sub>	<ul style="list-style-type: none"> <li>• Hardness is high</li> <li>• Excellent resistance to wear</li> <li>• Oxidation and corrosion resistant</li> </ul>	<ul style="list-style-type: none"> <li>• TiB<sub>2</sub> and Al<sub>3</sub>Ti are formed at the interface the during in-situ processing of the Al/TiB<sub>2</sub> composite.</li> <li>• The increased amount of brittle and needle-like Al<sub>3</sub>Ti compound reduces both the tensile and yield strengths.</li> <li>• The presence of coarser and higher volumes of Al<sub>3</sub>Ti compound may also contribute to the composite's continuous increase in modulus.</li> </ul>	[35,36]
8	ZrO <sub>2</sub>	<ul style="list-style-type: none"> <li>• Melting point is high</li> <li>• Fracture toughness is high</li> <li>• High wear resistance</li> <li>• Excellent mechanical properties</li> </ul>	<ul style="list-style-type: none"> <li>• At around 700 °C, there are no chemical reactions between the reinforcement particles of ZrO<sub>2</sub> and Al.</li> <li>• However, there is a possibility of Al<sub>2</sub>O<sub>3</sub> formation in the presence of oxygen and CuO formation in the presence of Cu as an alloying element.</li> </ul>	[37-39]
9	MoS <sub>2</sub>	<ul style="list-style-type: none"> <li>• Friction coefficient is low</li> <li>• Catalytic activity is good</li> <li>• Chemical stability and Thermal stability are better</li> </ul>	<ul style="list-style-type: none"> <li>• Depending on the process, the reaction products of Al and MoS<sub>2</sub> may be Al<sub>12</sub>Mo, Al<sub>5</sub>Mo, or Al<sub>2</sub>S<sub>3</sub>.</li> <li>• The Al<sub>2</sub>S<sub>3</sub> encourages strong bonding. Al<sub>12</sub>Mo has a higher elastic modulus than the Al matrix and is very stable. Al<sub>12</sub>Mo improves the mechanical properties of the Al matrix.</li> </ul>	[40,41]
10	ZrB <sub>2</sub>	<ul style="list-style-type: none"> <li>• Chemically inert</li> <li>• Wear resistance is high</li> <li>• Melting point is high</li> <li>• Strength is high at high temperature</li> <li>• Thermal and electrical conductivity are better</li> </ul>	<ul style="list-style-type: none"> <li>• Al<sub>3</sub>Zr and AlB<sub>2</sub> intermetallic compounds will likely form during the in-situ processing of Al/ZrB<sub>2</sub> composites.</li> <li>• The reaction temperature significantly impacts the morphology and size of Al<sub>3</sub>Zr particles. The presence of hard particles can improve strength, but an increase in hard particles can also decrease percentage elongation.</li> </ul>	[42-44]
11	CNT	<ul style="list-style-type: none"> <li>• Good ductility</li> <li>• Resistance to corrosion is good</li> <li>• Strength to weight ratio is high.</li> </ul>	<ul style="list-style-type: none"> <li>• Depending on the temperature, the interfacial reaction between the Al and the CNTs may form Al<sub>4</sub>C<sub>3</sub> at the interface between the Al and CNT layers.</li> <li>• The carbide formed improves the interfacial interaction between the CNTs and the Al layers. This also helps to improve the mechanical properties of the composite.</li> </ul>	[6,45]
12	Graphene	<ul style="list-style-type: none"> <li>• Strength to weight ratio is high.</li> </ul>	<ul style="list-style-type: none"> <li>• The formation of Al<sub>4</sub>C<sub>3</sub> intermetallic compound is possible as a result of the thermodynamically spontaneous reaction between Graphene and Al. The formation of Al<sub>4</sub>C<sub>3</sub> would significantly reduce the mechanical properties of the composite.</li> </ul>	[6,46]
13	Fly ash particles	<ul style="list-style-type: none"> <li>• Low density</li> <li>• Good wear and damping properties due to presence of oxides</li> </ul>	<ul style="list-style-type: none"> <li>• Fly ash contains a wide range of oxide combinations. There is no specific interfacial reaction reported in the literatures between Al and fly ash, but addition increases hardness while decreasing density in some cases.</li> </ul>	[4,47]

hardness, interfacial bonding between matrix and reinforcement and porosity depends on usage of different methods also. Most widely used manufacturing processes of MMCs are listed in Fig. 3. Total number of papers collected from science direct regarding metal matrix composites are approximately 1629 from the year 2011 to 2021. Search words are Metal Matrix Composites and MMCs. Detailed publication data is shown in Fig. 4.

Exponential growth is observed in use of stir casting process from year 2011 to 2021. Maximum number of papers published on MMC manufacturing are 804 and 504 by using stir casting and powder metallurgy methods respectively. Pie chart is also showing contribution of different methods in manufacturing of MMCs (Fig. 4(b)). Almost 50% of contribution is observed of stir casting process in MMC manufacturing. Hence, it is concluded that almost all over the globe research is progressing in the field of MMC by exploring stir casting process. MMC manufacturing methods are discussed in below section.

### 3.1. Powder Metallurgy (PM)

Many researchers have worked on fabrication of MMCs by powder metallurgy route to improve mechanical, thermal and electrical properties of alloys. It is the method of producing metal

and non-metal powders and utilizing them for manufacturing of composites [49]. Steps involved in PM are listed in Fig. 5. Sweet et al., [50] investigated microstructure and mechanical properties of hot upset forged 2xxx series Al alloy reinforced with AlN using powder metallurgy route. They manufactured high quality, defect free component and observed nearly full density of components (>99.5% theoretical). Sun et al., [51] also attempted to fabricate magnesium alloy composites using PM route to achieve uniform dispersion of reinforcement particles and refinement of matrix grains. They suggested to effectively maintain ball milling time as per required particle size for uniform mixing. Major limitation of powder metallurgy process is the high cost of metal powder compared to raw material used for other methods. It is also difficult to directly mass produce uniform density product.

### 3.2. Friction Stir Processing (FSP)

Friction stir processing method was adopted from friction stir welding. In this process matrix material is in the form of extruded or rolled plate. On this plate groove is machined to accommodate reinforcement particles. During FSP, non-consumable tool with shoulder and pin rotated and plunged into a metallic

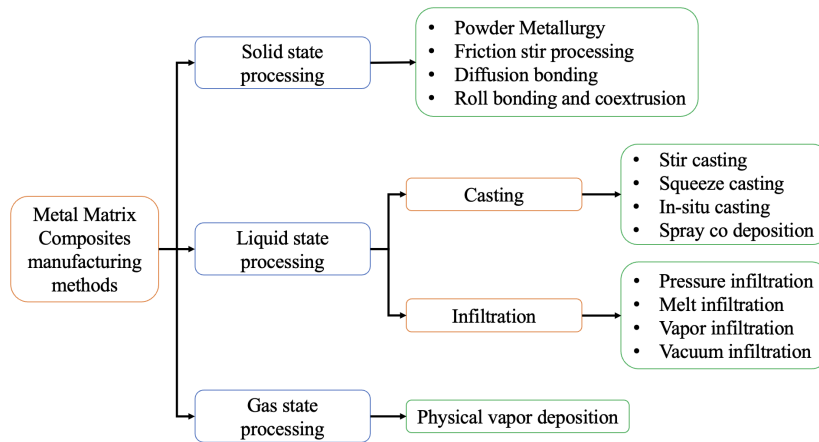


Fig. 3. Manufacturing processes for MMCs

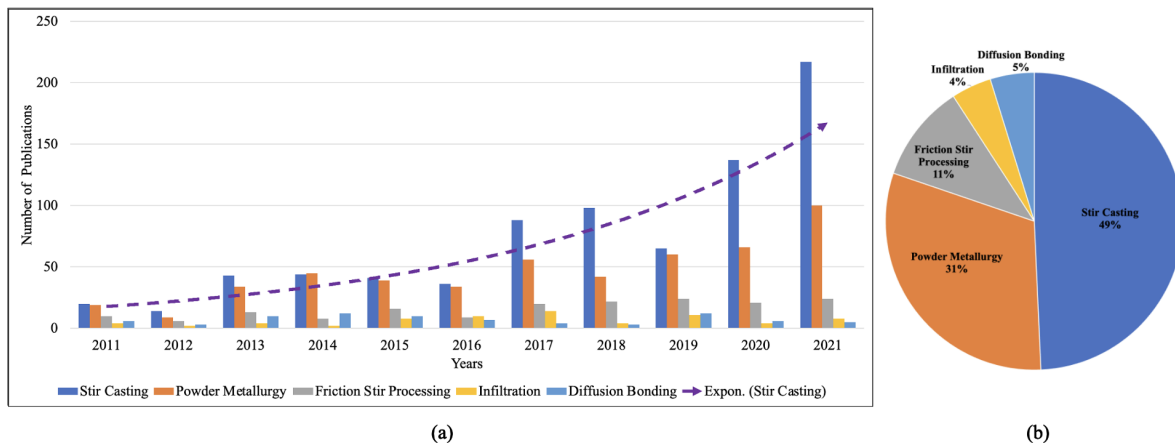


Fig. 4. Number of publications on manufacturing of metal matrix composites in the year 2011-2021

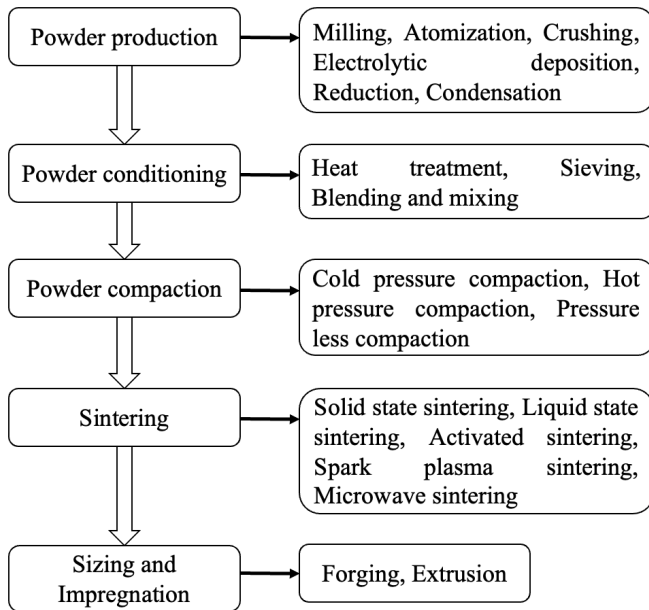


Fig. 5. Steps of powder metallurgy process

plate and then traversed along the surface of workpiece. Rotary and traverse motion between matrix and tool material result into rubbing action which generates heat due to friction and plasticizes material under the tool. Here, temperature increased is higher than recrystallization temperature of matrix material but less than melting temperature. During process, material is subjected to a combination of forging, extrusion and friction [52,53]. Because the entire process is completed in solid state, FSP is a type of solid state processing. During standard FSP there are chances of particle escape, to avoid this initially pin less tool is used. This tool plasticizes a thin layer of material and moves from one side to another and closes the groove opening. Further process is carried out using conventional tool. The stirring action of tool mixes the reinforcement particles with plasticized matrix material and creates composites [54]. Narimani et al., [55] reinforced  $TiB_2$  particles into Al alloy AA6063. They reported increase in tensile strength by about 70% higher than that of base material. FSP shows good potential for grain refinement, fabrication of surface and bulk metal matrix composites and micro structural homogenization. Use of FSP is limited due to expensive tooling involved and high frequency usage [14].

### 3.3. Diffusion bonding

Diffusion bonding involves stacking of matrix and reinforcement material on one another by tooling or even by hand. In this, reinforcements in the form of powder, wire or metal foil are used. After canning and evacuation, arranged matrix and reinforcements are hot pressed. This densification process is called diffusion bonding. Care to be taken to avoid their mutual contact and direct metal flows around monofilaments with a goal to achieve controlled reinforcement distribution and no porosity [56]. Chen et al., [57] used vacuum diffusion bonding

to prepare copper plated, sand blasted W and CuCrZr alloy. They mentioned important parameters for diffusion bonding such as bonding temperature, holding pressure and holding time. Major limitation of this process includes requirement of great care for surface preparation, high initial investment and limited size of component. This process is also difficult to use for mass production due to more bonding time [58].

### 3.4. Infiltration techniques

Infiltration means to enter into or through by filtering or permeating. In this method preform of reinforcement having pores is made. This preform is placed inside a crucible or container. On this preform liquid metal is poured. Liquid metal fills the pores of preform due to application of pressure and capillary action producing component having relatively high density [59,60]. Yamamoto et al., [61] fabricated AZ91/SiC fiber composite using low pressure infiltration method and added Al particles as infiltration promoters. Similarly, Bouzegzi et al., [62] studied microstructural and electrochemical properties of WC based MMC manufactured by infiltration method.

### 3.5. Stir casting

Casting is the primary and most commonly used method to fabricate MMCs. Casting involves melting and pouring of the material whereas stirring involves rotational movement of stirrer inside the melt for distributing reinforcement particles inside the melt. Stir casting setup is shown in Fig. 6. Furnace is used to melt the matrix material at required temperature. Most widely used furnaces are muffle furnace and resistance heating furnace. Feeder is used to supply reinforcement particles to the melt. Rate at which particles are fed into the crucible is important criteria. Reinforcement particles are preheated to certain temperature before mixing to improve wettability [63]. Next, stirrer is used to achieve uniform distribution of particles inside the melt. Furnace and motor can be connected to the control panel from where required temperature and RPM can be adjusted. With this setup gas supply arrangement is also provided. Inert gas supply is required for fabrication of reactive alloy MMCs such as Mg. After selecting suitable stirring time, melt is poured inside the die or mold. To avoid defects such as porosity, vacuum can also be maintained inside the mold and then pouring is done [6]. Nageswaran et al., [64] manufactured Cu/ $TiO_2$ /Gr hybrid composite using stir casting technique. Microstructural investigation revealed that particle distribution was uniform and agglomeration-free. They mentioned fine interfacial bonding between matrix and reinforcement. Stir casting process is most widely used to prepare MMCs of low melting point material because it is economical, simple, flexible and suitable for mass production. Limitation of this process involves difficulty in achieving homogeneity, high porosity and chances of reaction between matrix and reinforcement [65].

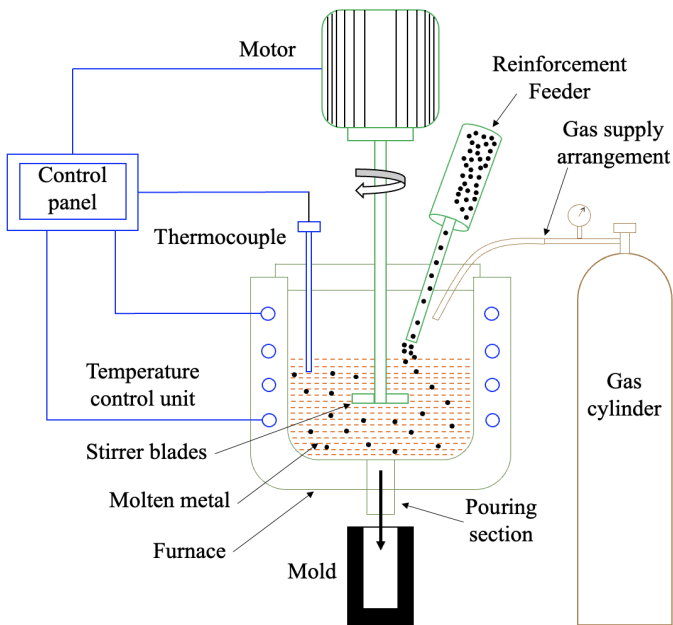


Fig. 6. Stir casting setup

In-situ fabrication of MMCs is the process in which required reinforcing phase is formed inside the matrix as a result of reaction from the melt during its cooling and solidification. Kumar et al., [42] developed AA5052/ZrB<sub>2</sub> composites by in-situ reaction of AA5052 alloy with two inorganic salts K<sub>2</sub>ZrF<sub>6</sub> and KBF<sub>4</sub> at a temperature of 860°C. They reported formation of nano and micro size ZrB<sub>2</sub> with uniform dispersion, a clear interface and good bonding. Selvam and Dinaharan [44] fabricated AA7075/ZrB<sub>2</sub> composites using in-situ method and same organic salts. They also reported good interfacial bonding between base alloy and reinforcements. In-situ formed ZrB<sub>2</sub> particulates improved microhardness and tensile strength of MMC compared to base alloy.

Squeeze casting can be considered as addition to stir casting process. In this process after pouring matrix and reinforcement

mixture, composition is subjected to pressure in die which improves mechanical properties and helps in grain refinement [66]. Kumar [67] fabricated Al7075/Agro waste composite using stir casting followed by squeeze casting method. Their results revealed that the manufactured composite is harder and possess high toughness and tensile strength. Squeeze casting is mostly performed after stir casting hence can also be considered as secondary improvement method for manufacturing of MMCs.

Considering all available MMC fabrication methods, stir casting is most reliable for manufacturing of Al MMCs, due to low melting point of Al and its alloy. This method is also simple, flexible and suitable for mass production. As many factors are affecting the quality and properties of MMCs, number of attempts have been made by researchers to improve the process and its outcomes. Al alloys were selected more by researchers due to its important properties such as light weight, high strength to weight ratio, wear resistance, corrosion resistance, low cost and sufficient viscosity of the melt. There are many parameters in stir casting which requires optimization for better quality MMC production. Stir casting parameters refers to the variables which affect properties and quality of final product. Main two parameters are design parameters and process parameters. Important parameters are listed as a cause and effect diagram in Fig. 7.

#### 4. Recent Studies on Effect of Stir Casting Process Parameters on Properties of Al MMCs

This section reviews recently used Al alloys and reinforcements by different researchers and various parameters considered with their effect on properties of Al MMCs. Kumar et al., [68] fabricated AA7178/ZrB<sub>2</sub> composite using stir casting process and reported homogeneous distribution of ZrB<sub>2</sub> particles and improvement in corrosion resistance than base alloy AA7178. They concluded that corrosion resistance, hardness and tensile

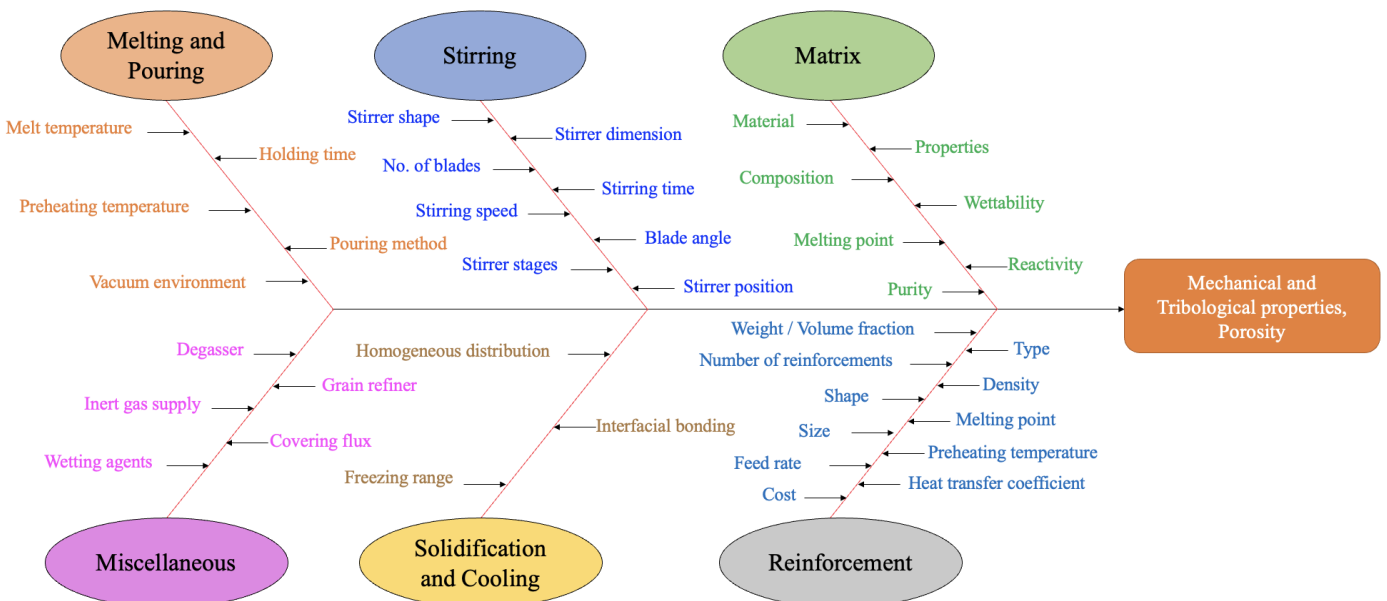


Fig. 7. Cause and effect diagram of stir casting parameters



strength increased gradually with the increase in weight percentages (0%, 5%, 10% and 15%) of particles. Also mentioned increment in hardness by 26% and tensile strength by 15% due to inclusion of 10 wt.% ZrB<sub>2</sub> particles in AA7178 matrix. Alizadeh et al., [69] fabricated Al5083/SiC composites by combining stir casting and squeeze casting process. Composites were having 20, 25 and 30 wt.% SiC. This combined route reduced porosities and improved particle distribution. Also, improvement in mechanical properties and wear resistance was observed. Akbar et al., [70] reinforced sea sand (2-6 wt.%) with AA6061 due to presence of SiO<sub>2</sub> and Fe<sub>3</sub>O<sub>4</sub> ceramic compounds. To improve wettability, electroless coating was applied on sea sand. They reported increase in hardness, tensile strength and decrease in porosity due to electroless coating. Increase in hardness and strength was due to addition of non-coated sea sand but addition of coated sea sand greater than 2 wt.% decreased hardness and strength of the composite. Adediran et al., [71] fabricated Al6061/waste glass particle (WGP) composites by varying weight proportion of WGP from 2 to 10% in the step of 2 wt.%. They mentioned reduction in elongation, impact energy and density with the increase in WGP from 0 to 10 wt.%. Increase in tensile properties observed up to 6 wt.% addition, then after tensile properties deteriorated. Highest compressive properties observed at 8 wt.% WGP addition while 10 wt.% addition reduced it. They further reported better wear resistance due to addition of WGP. Farajollahi et al., [72] studied microstructure, mechanical and tribological properties of AA2024/Ni MMC. They reported that addition of 1.5 wt.% Ni improved precipitation of Al-Cu-Mg near the interdendritic regions. Their amount reduced with further addition of Ni powder. Homogenization treatment precipitated needle shaped Al-Cu-Mg at the inner zone of dendrites and disappeared from the interdendritic region. Homogenization treatment and Ni powder addition resulted in Al<sub>3</sub>NiCu transformation from unreacted Ni and Al<sub>3</sub>Ni intermetallics. AA2024/3 wt.% Ni MMC reduced 13% coefficient of friction and 12% wear rate while increasing 42% of strength compared to base alloy. Balachandhar et al., [73] fabricated AA6061/Mg/rock dust composite and examined its surface roughness after turning process. They reported a 1% and 2% improvement in surface finish with the addition of AZ31 and rock dust, respectively. Babaremu et al., [74] fabricated AA8011/cow horn and corncob composites by varying reinforcement weight percentages from 5 to 20% in the steps of 5 wt.%. They achieved improvement in yield strength by 57%, in ultimate tensile strength by 52.6% and in hardness by 54.4% with the addition of 20 wt.% of cow horn and corncob. Zhu et al., [75] prepared AA6083/nano SiC (1 wt.%) composites and reported homogeneous distribution of nano SiC particles with grain refinement up to 30.55%. They also reported improvement in yield strength, ultimate tensile strength and elongation by 12.16%, 8.92% and 12.60% respectively compared to base alloy. Further squeeze casting improved yield strength by 43.18%, ultimate tensile strength by 29.81% and elongation by 226.28% compared to only stir cast composites. Mohanavel et al., [76] fabricated AA6351/Si<sub>3</sub>N<sub>4</sub> composites by varying wt.% of Si<sub>3</sub>N<sub>4</sub> from 1 to 3% in the steps of 1 wt.%. They reported

uniform dispersion of Si<sub>3</sub>N<sub>4</sub> in the matrix and improvement in mechanical properties of composites. Addition of 3 wt.% Si<sub>3</sub>N<sub>4</sub> improved microhardness by 40.30% and decreased wear rate. Further they also mentioned increase in compressive strength with the increase in Si<sub>3</sub>N<sub>4</sub> wt.%. They concluded that the AA6351 having 3 wt.% Si<sub>3</sub>N<sub>4</sub> composites had the highest mechanical and wear properties among all the fabricated composites. Sahoo et al., [77] fabricated AA6061/SiC/hBN hybrid composites. Microstructural study revealed increase in density by 6.52% due to homogeneous dispersion of particles. They also studied wear properties of composite Al/hBN (5 wt.%) /SiC (4 wt.%) by using pin-on-disc method and reported that decrease in wear loss was due to hBN particles addition. Gudipudi et al., [78] prepared AA6061/B<sub>4</sub>C composites. They achieved homogeneous B<sub>4</sub>C dispersion and grain refinement at 4 wt.% B<sub>4</sub>C addition. They also reported increase in specific ultimate tensile strength by 36.32% and increase in compressive strength by 43.92%. Vickers hardness improved by 53.41% and Brinell hardness increased by 50.89% due to 4 wt.% B<sub>4</sub>C addition compared to base alloy. Shayan et al., [79] fabricated composite by reinforcing nano SiO<sub>2</sub> (0.5%) and TiO<sub>2</sub> (1%) in AA2024 alloy. It was observed that addition of nano particles reduced grain size. The study of mechanical properties revealed increase in yield strength by 7%, ultimate tensile strength by 36% and hardness by 30% compared to base alloy. They reported evidence of agglomeration of nano particles on the fractured surface of composites properties with the addition of 1 vol.% of SiO<sub>2</sub> compared to that of 0.5 vol.% of SiO<sub>2</sub>. Subramaniam et al., [80] fabricated Al7075/B<sub>4</sub>C/coconut shell fly ash (CSFA) composites by varying wt.% of B<sub>4</sub>C from 3 to 12 wt.% in the steps of 3 wt.% and keeping 3 wt.% CSFA constant. They reported increase in hardness by 33% due to addition of 12 wt.% B<sub>4</sub>C and 3 wt.% CSFA. Addition of 9 wt.% B<sub>4</sub>C and 3 wt.% CSFA improved tensile strength of composite by 66% and impact energy up to 2.3 J compared to base alloy. Further increase in wt.% of reinforcements reduced impact energy and tensile strength. Addition of B<sub>4</sub>C and CSFA reduced elongation of composite. Selvam et al., [81] fabricated in-situ AA6061/Al<sub>2</sub>O<sub>3</sub>/TiB<sub>2</sub> composites using boric acid powder and titanium. They reported uniform distribution of Al<sub>2</sub>O<sub>3</sub> and TiB<sub>2</sub> with good interfacial bonding. Al<sub>2</sub>O<sub>3</sub> particles were having spherical shape while TiB<sub>2</sub> particles were having hexagonal and cubic shapes. In-situ formation of Al<sub>2</sub>O<sub>3</sub> and TiB<sub>2</sub>, refined the grains of matrix to 14 μm at 15 wt.% compared to 103 μm at 0 wt.%. They also reported improvement in microhardness and tensile strength compared to that of base alloy. Reported tensile strength and micro hardness values at 15 wt.% were 287 MPa and 122 HV respectively.

Turan et al., [82] added 1 wt.% fraction of 8 to 18 nm diameter multiwalled carbon nanotube (MWCNT) and 1.5 μm diameter graphene nanoplatelets (GNP) to the AlSi18CuNiMg alloy. Stir casting and semi powder metallurgy was adopted for composite fabrication. Graphene addition showed improvement in tribological properties. Addition of nano carbon material improved hardness of base alloy. They concluded that factors affecting wear rate were material content, sliding speed and ap-

plied load. Sharma et al., [83] prepared Al-Mg-Si-T6 composite with the reinforcement of 6  $\mu\text{m}$  black SiC and 28  $\mu\text{m}$  muscovite. Muscovite is hydrated aluminium potassium silicate particulates. They varied weight percentage of muscovite (2, 3 and 4 wt.%) and kept 5 wt.% SiC constant. Increase in muscovite percentage improved wear resistance. The higher hardness was achieved with the use of 5 wt.% SiC and 3 wt.% muscovite. Microstructural study revealed cluster formation. Increase in tensile strength was observed with the addition of 2 to 3 wt.% composition but it was decreased after the addition of 4 wt.% muscovite. Kumar et al., [84] fabricated Al-Mg-Si-T6/industrial fly ash composites. They aimed to achieve high strength and low density for automobile and aerospace applications. They varied wt.% from 5 to 20% in the step of 5 wt.%. Addition of 10 wt.% fly ash improved properties better than other composites. Further, they reinforced B<sub>4</sub>C (2.5%, 5%, 7.5%) and fly ash (5 wt.%) with the base alloy. They reported that 5 wt.% fly ash and 5 wt.% B<sub>4</sub>C reinforced composites showed improvement in tensile strength, hardness and compressive strength by 18.7%, 11.3% and 38.6% respectively compared to base alloy. Mann & Pandey [30] investigated effect of Al<sub>2</sub>O<sub>3</sub> reinforcement on the wearing characteristics of LM30 aluminium alloy. They prepared composites with different size of particles and varying weight percentages from 5 to 20 wt.%. After stir casting, they observed uniform distribution and decrease in wear rate with the addition of reinforcement. Rao et al., [85] reinforced Al-Cu alloy with MoS<sub>2</sub> using stir casting process. MoS<sub>2</sub> was added at three different weight fractions 2 wt.%, 4 wt.% and 6 wt.%. Addition up to 4 wt.% showed increase in tensile strength and micro hardness. But 6 wt.% addition of reinforcement leads to decrease in these properties. Microstructural study revealed homogeneous distribution of particles and fine grain refinement. These leads to improvement in density. Wang et al., [86] reinforced Ni coated nano Al<sub>2</sub>O<sub>3</sub> particles in A356 alloy using combination of stir casting and equal channel angle semi solid extrusion (ECASE). They reported that Ni coating could break nano particle clustering and particle located on grain boundary distributed more uniformly having grain size 63 nm. Use of ECASE further refined grain size to 23  $\mu\text{m}$  and improved nano particle distribution. Fabricated nano MMC exhibited 1.2 to 2.5 times improvement in ductility and strength compared to MMC fabricated by stir casting. ECASE eliminated the intergranular defects and improved the grain boundary bonding. Wettability improvement between matrix and reinforcement during melting can be improved by using Ni coating surface modification process. Hu et al., [87] prepared Al/B<sub>4</sub>C/Ti composite by adding 12 wt.% B<sub>4</sub>C and 3 wt.% Ti. They reported formation of Al<sub>3</sub>BC intermetallic phase at the interface of composites. They mentioned properties of Al<sub>3</sub>BC such as brittle, high hardness, elastic anisotropy, good thermal stability and poor dynamic stability. Al<sub>3</sub>BC had semiconductor properties and its bonding was ionic, covalent and metallic. They also studied density functional theory (DFT) for all the properties.

Aigbodion et al., [88] produced composites having Al-3.7%Cu-1.4%Mg with 1.5 wt.% Rice husk ash nanoparticles using the modified stir casting and double feeding method. They

suggested to use fabricated composite for impeller application based on tested tensile strength, factor of safety and corrosion rate. They mentioned that the yield strength of the material is lower than the maximum Von Misses' stress. Corrosion rate reduced by 23.57% when compared with steel impeller. They finally suggested that proposed method and material is suitable for pump impeller production. The speed was found to be the most influential factor on surface roughness during turning. Singh & Pal [89] fabricated aluminium MMCs by reinforcing SiC particles, TiO<sub>2</sub> coated SiC particles and Li<sub>4</sub>Ti<sub>5</sub>O<sub>12</sub> coated SiC particles via stir casting process under vacuum. Due to reinforcement, significant amount of grain refinement was observed. They reported highest value of damping capacity and storage modulus for Li<sub>4</sub>Ti<sub>5</sub>O<sub>12</sub> coated SiC/Al MMC compared to other fabricated MMCs. Velavan et al., [90] added 3, 4, 5, 6 wt.% Mica, while maintaining 10 wt.% B<sub>4</sub>C. They reported improvement in mechanical properties after mixing 3 wt.% of mica. They also reported decrease in impact strength upon inclusion of more than 3 wt.% Mica. They suggested to use fabricated MMC for automobile related sheet forming operations. Zhang et al., [91] reported that vortex free high speed electromagnetic mechanical stirring (VFHSC) could reduce the porosity to about 0.036 vol.% using 2200 – 2700 rpm for Al-1.5 wt.% Si/Al<sub>2</sub>O<sub>3</sub> (3  $\mu\text{m}$ ) composite fabrication. They also reported increase in tensile strength, hardness and decrease in wear rate by 73.6%, 35% and 92.6%, due to addition of 5 vol.% Al<sub>2</sub>O<sub>3</sub>. Zhang et al., [92] fabricated Al-1.5 wt.% Si/SiC composite using VFHSC method. They reported uniform distribution of particles and reduction in porosity to less than 0.04 vol.%. They also mentioned increase in tensile strength, hardness and decrease in wear rate by 64.9%, 30% and 92.4% respectively, due to addition of 8 vol.% of SiC particles. Ramadoss et al., [93] fabricated Al/B<sub>4</sub>C/BN composites by keeping 3 wt.% of BN constant and varying wt.% of B<sub>4</sub>C from 3 to 9% in the step of 3 wt.% to focus for marine applications. They reported uniform dispersion of particles in the MMC and formation of intermetallic phases such as Al<sub>3</sub>BC, AlB<sub>12</sub> and AlN. They also mentioned increase in tensile strength, hardness and decrease in corrosion rate compared to that of base alloy. Christy et al., [94] fabricated recycled Al alloy/Al<sub>2</sub>O<sub>3</sub> composites using stir-squeeze casting process. They used Taguchi grey relational analysis method to optimize stirring speed and squeeze process parameters such as time, pressure and die preheating temperature. They reported optimized parameters such as 525 rpm stirring speed, 100 MPa squeeze pressure, 45 second squeeze time and 250°C die temperature. Karthikeyan et al., [95] reinforced ZrO<sub>2</sub> with 3 to 12 wt.% in the step of 3 wt.%. Increase in tensile and compressive strength observed with addition of ZrO<sub>2</sub>. Further, increase in heat transfer rate, efficiency and effectiveness was observed for pin fin with increase in ZrO<sub>2</sub>. Highest values were observed for LM6/12 wt.% ZrO<sub>2</sub> composite. Faisal et al., [96] reported improvement in hardness and tensile strength with the addition of B<sub>4</sub>C in LM6 alloy but 8% B<sub>4</sub>C addition showed reduction in tensile strength. Gr was added to improve wear properties. LM6/7 wt.% B<sub>4</sub>C/2 wt.% Gr composite improved tensile strength as well as wear properties. Xue et al., [97]

studied effect of addition of CeO<sub>2</sub> on microstructure and mechanical properties of Al composites. Addition of 0.5 wt.% CeO<sub>2</sub> improved yield strength, ultimate tensile strength and elastic limit by 14.1%, 8.7% and 39.1% than those of composite without CeO<sub>2</sub>. Addition of Cerium improved wettability of TiB<sub>2</sub> particles in Al melt due to reduction in surface tension of aluminium. Optimum dispersion, refinement and modification observed with addition of 0.5 wt.% CeO<sub>2</sub>. Pramod et al., [98] studied effect of addition of Scandium (Sc) on microstructural and mechanical properties of A356/5 wt.% TiB<sub>2</sub>. Sc addition reduced Si particle size to 2 µm. Si morphology changed to globular from fibrous after T6 heat treatment. They reported homogeneous particle dispersion and reduction in secondary dendrite arm spacing (SDAS) by 65% due to addition of 0.4 wt.% Sc. They also reported increase in yield strength, ultimate tensile strength, ductility and hardness by 33%, 24%, 7% and 30% respectively compared to base alloy. T6 heat treatment showed improvement in ultimate tensile strength by 44% and yield strength by 98% for A356/5 wt.% TiB<sub>2</sub>/0.4 wt.% Sc composite compared to A356 base alloy. Ma & Wang [99] studied the effect of T6 heat treatment and strontium (Sr) addition on mechanical and microstructural properties of in-situ A356/5 vol.% Al<sub>3</sub>Ti composite. Addition of 0.02 wt.% Sr addition reduced particle size and aspect ratio of Si particulates without affecting Al<sub>3</sub>Ti particulates. Al<sub>3</sub>Ti particulates observed in blocky morphology with average size of 5 to 6 µm. Addition of Al<sub>3</sub>Ti improved yield strength but reduced elongation. Combination of Al<sub>3</sub>Ti and Sr improved strength and ductility both due to modification of eutectic Si particulates. Microstructure based representative volume element (RVE) simulation revealed about the microscale damage evolution of the material. Krishnan et al., [100] fabricated the composites using scrap Al alloy and Al<sub>2</sub>O<sub>3</sub>. They reported formation of eutectic Si phase of the matrix due

to reinforcement. They concluded decrease in porosity by 7.3%, abrasive wear loss of 0.11 mg, higher hardness of 58.5 BHN, second highest ultimate tensile strength of 125 MPa and ultimate compressive strength of 312 MPa among the fabricated composites. Idrisi & Mourad [101] used ultrasonic assisted stir casting process to fabricate composites by varying wt.% of SiC (3, 5, 8 and 10 wt.%). The size of particles used was 40 µm. Use of ultrasonic probe resulted in uniform dispersion of SiC particles. They reported improvement in mechanical and physical properties with the use of ultrasonic assisted stir casting process compared to only mechanical stirring. Suthar & Patel [102] fabricated pure Al/B<sub>4</sub>C (10 wt.%)/Ti (0.2 wt.%)/graphite (5 wt.%) composites. They reported that high tensile strength and low porosity can be achieved by optimizing stirring time, stirring speed, reinforcement amount and preheating temperature. 650 rpm stirring speed and 12 minutes stirring time helped to achieve low porosity. Degassing and fluxing reduced porosity below 3%. They also suggested to use automatic stirring process for uniform dispersion of particles compared to manual stirring. Permanent mould, degassing, fluxing and automatic stirring improved tensile strength above 150 MPa due to uniform particle distribution and removal of slag and air entrapment.

### 5. Effect of Stirrer Design Parameters on Particle Distribution in Al MMCs Fabrication

Stirrer design parameters involves stirrer shape, stirrer dimension, stirrer stages, blade design and blade angles. There have been very few articles that have focused on determining the best stirring parameters to improve mechanical characteristics and microstructure. TABLE 2 has a list of them. Various stirrer designs reported in publications are redrawn in Fig. 8.

TABLE 2

Review ongoing research to study the effect of stirring parameters on the structure and properties of Al MMCs

Sr. No.	MMCs	Parameters	Effect on Microstructure	Effect on Properties	References
1	LM25/ SiC	Stirrer Design (4 blade stirrer) (Blade angle), Stirrer Position, Stirrer speed	<ul style="list-style-type: none"> <li>A uniform distribution of particles in the microstructure was observed at a stirrer position of 40 mm from the base.</li> <li>The lowest particle distribution was observed at 90° blade angle because melt would not experience lift.</li> <li>In contrast, a 45° blade angle resulted in uniform particle distribution at the bottom, top, and middle positions. They discovered that stirrer geometry has the greatest influence on cast sample properties.</li> </ul>	<ul style="list-style-type: none"> <li>Highest strength was observed for 45° blade angle, 40 mm stirrer position from base and 400 rpm stirrer speed due to uniform particle distribution in the poured slurry.</li> </ul>	[103]
2	AA8011/ SiC	Stirrer Design (Blade angle, Turbine stirrer), Stirrer position, Stirring speed	<ul style="list-style-type: none"> <li>Streak photography was used to visualise the stirring experiment using a glycerol and graphite particle combination.</li> <li>High vortex pressure produced by a 90° blade angle caused void formation, clustering, and non-uniform distribution in samples.</li> <li>A 45° blade angle produced a better flow pattern and uniform particle distribution, whereas a 90° blade angle produced poor particle distribution and particle agglomeration.</li> <li>They recommended a stirring speed of less than or equal to 250 rpm, a blade angle of 45°, and a stirrer position of 40% from the base for uniform particle distribution.</li> </ul>	<ul style="list-style-type: none"> <li>Some samples' hardness was reported to have decreased due to the presence of porosity.</li> <li>The main reason stated for the decrease in hardness was the increased blade angle and stirring speed.</li> </ul>	[104]

3	Waste Al/ Al <sub>2</sub> O <sub>3</sub>	Stirrer Design (3 blade radial flat, radial curved, radial chamfered, 4 blade Mixer flat, 3 blade Axial chamfered)	<ul style="list-style-type: none"> <li>• Uniform particle distribution was noticed in the case of the four blade Mixer flat stirrer, and simulation supported this.</li> <li>• The four bladed mixed flat stirrer also showed smaller pore sizes and pores were fewer and grain size was also small.</li> </ul>	<ul style="list-style-type: none"> <li>• Maximum hardness was achieved with the use of 4 bladed mixed flat stirrer.</li> <li>• Same stirrer provided 206 MPa tensile strength and 642 MPa compressive strength which were highest among all the stirrers used.</li> </ul>	[105]
4	AA6061/ MWCNT	Stirrer Design (Four bladed, U-shaped, Four bladed disc turbine stirrer)	<ul style="list-style-type: none"> <li>• Due to controlled vortex formation, a four-bladed disc turbine stirrer distributed reinforcement particles homogeneously and uniformly.</li> <li>• They also reported non dendrite structure formation.</li> </ul>	<ul style="list-style-type: none"> <li>• The work is solely concerned with microstructure.</li> </ul>	[106]
5	AA6061/ Si/Mg/Cu	Stirrer Design (Four side paddle blade, Alternate paddle blade, Helical blade)	<ul style="list-style-type: none"> <li>• In the alternate paddle blade design, SiC particles were properly mixed with matrix, and particle scattering was also better than in the four-sided paddle blade.</li> <li>• They also reported that grain boundaries were discontinuous and that the gap between dendrites had grown.</li> <li>• They also reported a porosity defect in all of the samples..</li> </ul>	<ul style="list-style-type: none"> <li>• Tensile strength was higher in samples prepared with an alternate paddle blade design. The tensile strength and ductility of helical spring samples were lower.</li> <li>• The hardest samples were those prepared with a four-sided paddle blade and an alternate paddle blade design.</li> <li>• The hardness of samples prepared with a helical blade was low.</li> </ul>	[107]
6	AA8011/ SiC	Stirrer Design (Blade angle), Stirrer position, Stirring speed	<ul style="list-style-type: none"> <li>• A 10% reinforcement volume fraction, a 40% stirrer position from the base, a 45° blade angle, and a 10 minute stirring time resulted in homogeneous distribution.</li> </ul>	<ul style="list-style-type: none"> <li>• The optimal pressure for uniform particle distribution and an effective flow pattern was reported to be in the range of 15 to 26 Pa.</li> <li>• A sample with a 10% volume fraction of reinforcement, 40% stirrer position from the base, 45° blade angle, and 10 minute stirring time resulted in higher tensile strength, hardness, and a lower wear rate.</li> </ul>	[108]
7	AA6061/ TiC	Stirrer blade angle, Stirrer speed, Stirring time	<ul style="list-style-type: none"> <li>• Homogeneous particle distribution was observed at a blade angle of 30°, a stirring speed of 300 rpm, and a stirring time of 15 minutes.</li> </ul>	<ul style="list-style-type: none"> <li>• The highest tensile strength and micro hardness were achieved by using a blade angle of 30°, a stirring speed of 300 rpm, and a stirring time of 15 minutes.</li> <li>• They concluded that, in decreasing order, blade angle, stirring speed, and stirring time affect tensile strength and microhardness.</li> </ul>	[109]
8	AA6061/ TiC	Stirrer Design (Blade angle), Stirrer speed, Stirring time	<ul style="list-style-type: none"> <li>• They reported better particle distribution at 300 rpm stirring speed.</li> <li>• Particle distribution was uniform at 30° blade angle. At 60° blade angle, there were very few particles on top and a uniform particle distribution on the bottom.</li> <li>• They were also concerned about porosity.</li> </ul>	<ul style="list-style-type: none"> <li>• UTS improved with increasing stirring speed up to 300 rpm, after which it decreased.</li> <li>• Reported improvement in UTS as stirring time was increased up to 15 minutes, after which it began to decrease. UTS was increased up to a blade angle of 30°, after which it was reduced.</li> <li>• This could be due to faster vortex formation and more air entrapment for longer stirring time.</li> </ul>	[110]

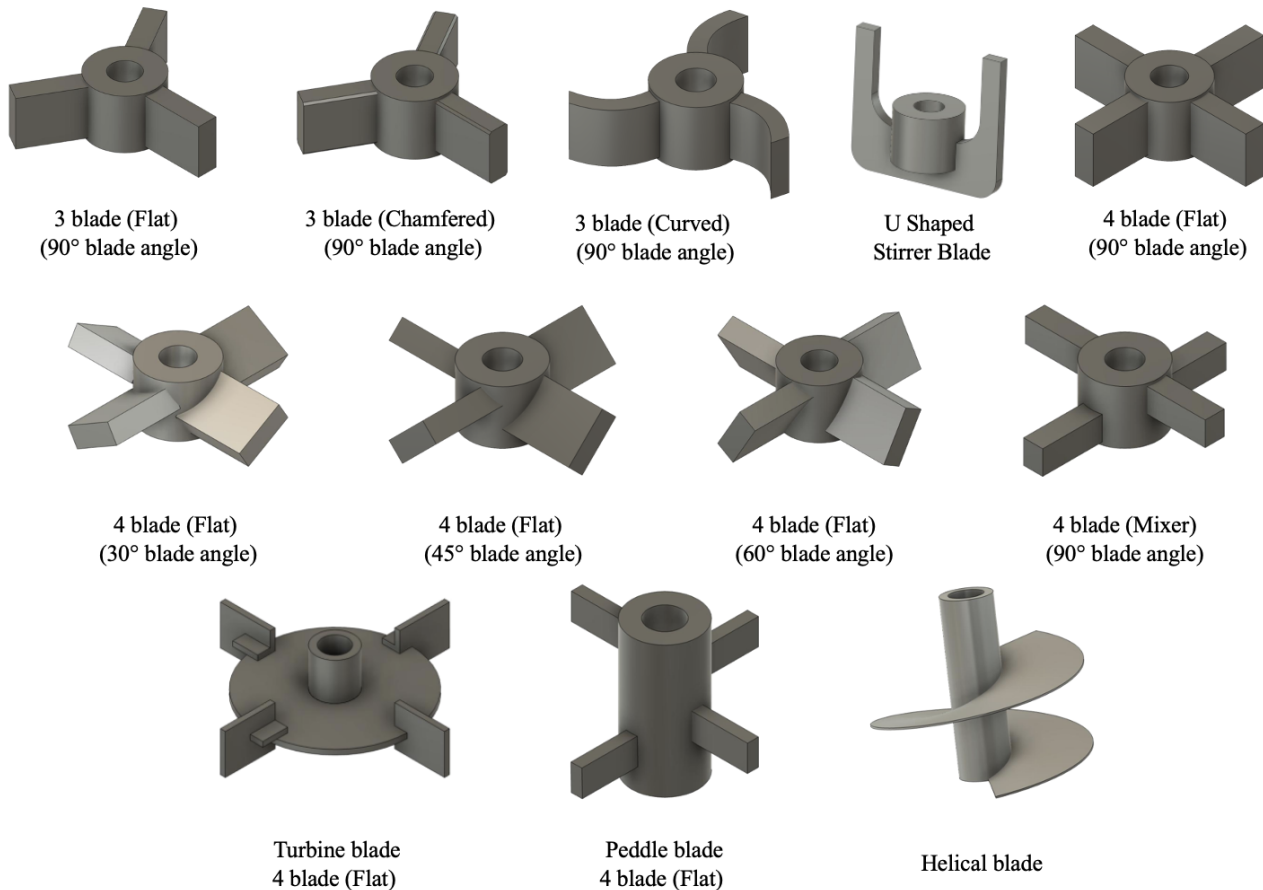


Fig. 8. Various stirrer designs reported in publications

Quality of fabricated part majorly depends on particle distribution. Particle distribution is significantly affected by flow behaviour of fluid. As stir casting process is performed in closed environment, it is difficult to visualize the process. Some of the researchers have attempted to simulate the stirring process to study the effect of stirring parameters on flow behaviour and particle distribution. Bui et al., [111] developed three dimensional two phase flow, steady state model to study the volume fraction distribution and flow field for processing of Al/SiC composite in molten state. They first performed simulation on water model and reported that smaller particle size will be helpful for better mixing. They suggested to use Al/SiC composite simulation to study various combination of stirring speed and rotational direction. For modelling, important work was the sedimentation of particles. For sedimentation understanding, they removed gravity effect and particle phase was considered to be non-viscous having very high viscosity. Hence, simulation can be considered as one of the ways to understand effect of blade design on flow behaviour and particle distribution. Rohatgi et al., [112] used gravimetry technique for mixing of two phase slurries in the model of SiC-water system to determine effect of stirrer geometry and baffles on the distribution of SiC in the mixture. They used three blade stirrer and varied blade angle and stirring speed. They reported that distribution of particles was improved in the presence of baffles. Biswas et al., [113] used sand water slurry system to study the effect of design parameters such as

stirrer type, stirrer angle, blade type, rotation direction, number of stages of stirrer and number of blades. They did work to understand dynamics behind liquid metallurgy technique. Based on experimental data, they suggested that propeller type stirrer is more suitable than hollow piped stirrer. They recommended a blade angle of  $30^\circ$  with respect to the stirrer shaft axis. The use of anticlockwise rotation showed better performance than clockwise. Operating parameters influences air entrapment, piping and particle distribution. The optimal position of the stirrer from the base was reported to be 30 mm. Naher et al., [114] performed visualization experiment using water glycerol system to study effect of stirring speed, stirrer height and stirrer type on the particle distribution. Results revealed that stirring speed and blade angle majorly influenced particle distribution. Naher et al., [115] also performed experimental and computational analysis to study effect of viscosity on particle distribution during Al/SiC MMC fabrication. Viscosities values used were 1 mPas and 300 mPas. They reported suitable stirring speed 200 rpm and stirring time of 14 to 170 s for lower viscosity fluids. For higher viscous systems, a stirring speed of 300 rpm and a stirring time of 540 to more than 3920 seconds was recommended. Suspension of particles was reported for few seconds in lower viscosity fluid and about an hour for higher viscosity fluid.

Su et al., [116] performed experimental and computational analysis to study effect of viscosity on particle distribution and flow patterns for different stirrer geometry, stirring speed and stir-

rer position using ANSYS Fluent simulation package. They used multiphase  $k-\varepsilon$  turbulence model for flow prediction. They varied blade dimension by using  $d/D$  ratio. Here,  $d$  indicates impeller diameter and  $D$  indicates crucible diameter. For uniform particle distribution they suggested use of multistage stirrer, 100 rpm stirring speed,  $30^\circ$  blade angle and 0.55  $d/D$  value. Kumar et al., [117] simulated stir casting process to study the effect of stirring speed on particle distribution. They kept viscosity 4.4 mPas and blade angle  $60^\circ$  constant. Two stirring speed selected was 200 rpm and 400 rpm for stirring simulation. Simulation was performed using multiphase model in ANSYS Fluent package. From simulation result they concluded that stirring speed greatly affected the particle distribution and for better particle distribution 400 rpm speed was suggested. Prasad et al., [118] simulated stir casting process of Al MMC to compare it with experimental procedure. They used ANSYS Fluent package to simulate the process. The  $k-\varepsilon$  turbulence model was selected and further conditions were defined. They analysed that shearing rate in the fluid domain directly affected the mixing effectiveness. They also suggested relationship between shear rate and particle dispersion time. Yamamoto et al., [13] investigated flow behaviour for different impeller design during stirring of molten Al. They used impeller having twisted blade. Particle Image Velocimetry (PIV) and numerical simulation using water model were used to study effect of twisting blade angle on flow pattern. For simulation they used open-source software OpenFOAM. Solver used was PimpleDynFoam. They reported that increase in twisting angle reduces gap between adjacent blades which reduces the amount of sucked liquid. Impeller with  $30^\circ$  twist angle created strong downward flow. They proposed that future research be directed at trailing vortices, gas bubbles and power number in order to optimise this process. Rajendra et al., [119] simulated stir casting process by varying blade angle and stirring speed. Simulation was performed using multiphase  $k-\omega$  model and volume of fluid method in ANSYS Fluent package. They mentioned that uniform mixing was achieved using 300 rpm speed and  $30^\circ$  blade angle at viscosity of 3.2 mPa-s. After 57 seconds, reinforcement particles started to stabilize. They concluded that blade angle and stirring speed were majorly affecting particle distribution inside the molten metal.

### 5.1. ANSYS Fluent – Stir Casting Simulation Methods

According to a review of the literature, ANSYS fluent is mostly used by researchers for stir casting process simulation as it has been commercially adopted by many industries. This tool is simple to use and has a wide range of applications. OpenFOAM, Z-Cast, MAGMA and Pro-Cast software are limited in use due to the complexity of the multi-physics module when compared to ANSYS fluent. In ANSYS Fluent, for simulation, models selected by researchers were  $k-\varepsilon$  model and  $k-\omega$  model. Mainly this models solves for Reynolds Average Navier Stokes (RANS) equations. Most important step during simulation setup is the model selection. In stir casting, mixing process involves rotation

of fluid using impeller. In such situation, Reynolds number will help to depict the nature of flow. For any flow Reynolds number is defined as,

$$Re = \frac{\rho V D}{\mu} \quad (1)$$

Here,  $\rho$  is the density,  $V$  is the velocity of impeller,  $D$  is diameter of the container and  $\mu$  is the dynamic viscosity of the fluid. If  $Re < 20$  then flow behaviour will be laminar and if  $Re > 10000$  then flow behaviour will be turbulent [120]. Multiphysics module is required when more than one phases are involved in the process. In most cases, phase is considered to be one of the type matters, such as solid, liquid or gas. Multiphase module includes homogeneous model and inhomogeneous model. Volume of fluid (VOF), Mixture and Wet steam are homogeneous models and Eulerian is inhomogeneous model. Turbulent flows are best described by fluctuating velocity fields. These variations combine transportable quantities such as species concentration and energy and cause them to vary as well. Since these variations might be of low magnitude and high frequency, simulating them directly in engineering calculations is computationally costly. Instead, the instantaneous governing equations can be time averaged or otherwise adjusted to eliminate the resolution of small scales, yielding a new set of equations that are computationally easier to solve. RANS equations are used by engineers for the flow simulations. Equations are solved for time averaged flow behaviour and the magnitude of turbulent fluctuations. RANS equation is considered as below:

$$\begin{aligned} \frac{\partial(\rho u_i)}{\partial t} + \frac{\partial(\rho u_i u_j)}{\partial x_j} = \\ = -\frac{\partial p}{\partial x_i} + \frac{\partial}{\partial x_j} \left[ \mu \left( \frac{\partial u_i}{\partial x_j} + \frac{\partial u_j}{\partial x_i} \right) \right] + \frac{\partial}{\partial x_j} \left( -\overline{\rho u_i u_j} \right) \end{aligned} \quad (2)$$

Here,  $-\overline{\rho u_i u_j}$  represents the effect of turbulence. This is called Reynolds Stress. Reynolds stress is modelled using Boussinesq approach. It is used in  $k-\varepsilon$  model and  $k-\omega$  model.

$$-\overline{\rho u_i u_j} = \mu_t \left( \frac{\partial u_i}{\partial x_j} + \frac{\partial u_j}{\partial x_i} \right) - \frac{2}{3} \left( \rho k + \mu_t \frac{u_k}{x_k} \right) \delta_{ij} \quad (3)$$

Here,  $u$  indicates instantaneous velocity which is also equal to  $\bar{u} + u'$ ,  $\bar{u}$  is time average velocity,  $u'$  is fluctuating velocity,  $\mu$  is dynamic viscosity and  $\mu_t$  indicates eddy viscosity (Turbulent viscosity).

Standard  $k-\varepsilon$  model assumes the existence of isotropic turbulence and spectral equilibrium. It is primarily a high Reynolds number model. Equation for kinetic turbulent energy ( $k$ ) and turbulent dissipation rate ( $\varepsilon$ ) are mentioned below:

$$\begin{aligned} \frac{\partial(\rho k)}{\partial t} + \frac{\partial(\rho k u_i)}{\partial x_i} = \\ = \frac{\partial}{\partial x_j} \left[ \left( \mu + \frac{\mu_t}{\sigma_k} \right) \frac{\partial k}{\partial x_j} \right] + G_k + G_b - \rho \varepsilon - Y_M + S_k \end{aligned} \quad (4)$$

$$\frac{\partial(\rho\varepsilon)}{\partial t} + \frac{\partial(\rho\varepsilon u_j)}{\partial x_j} = \frac{\partial}{\partial x_j} \left[ \left( \mu + \frac{\mu_t}{\sigma_\varepsilon} \right) \frac{\partial \varepsilon}{\partial x_j} \right] + C_{\varepsilon 1} \frac{\varepsilon}{k} (G_k + C_{\varepsilon 3} G_b) - C_{\varepsilon 2} \rho \frac{\varepsilon^2}{k} + S_\varepsilon \quad (5)$$

Here,  $u_i$  indicates velocity component in corresponding direction,  $G_k$  represents the generation of turbulence kinetic energy due to mean velocity gradients,  $G_b$  represents the generation of turbulence kinetic energy due to buoyancy,  $Y_M$  indicates contribution of the fluctuating dilatation in compressible turbulence to the overall dissipation rate,  $C_{\varepsilon 1}$ ,  $C_{\varepsilon 2}$  and  $C_{\varepsilon 3}$  are constants,  $\sigma_\varepsilon$  is the turbulent Prandtl numbers for  $\varepsilon$ ,  $\sigma_k$  is the turbulent Prandtl numbers for  $k$ ,  $S_\varepsilon$  and  $S_k$  are user defined source terms which can represent pressure gradient, gravity or any other body forces imposed or removed from the phase. The turbulent viscosity or eddy viscosity,  $\mu_t$ , is computed as follows:

$$\mu_t = \frac{\rho C_\mu k^2}{\varepsilon} \quad (6)$$

Values of different constants for  $k$ - $\varepsilon$  model are  $C_\mu = 0.09$ ,  $C_{\varepsilon 1} = 1.55$ ,  $C_{\varepsilon 2} = 2.0$ ,  $\sigma_k = 1$ ,  $\sigma_\varepsilon = 1.3$ .

This model has difficulty to consider streamline curvature, body-force effects and rotational strains. It has also problem at close wall flow handling, resolving vortexes, large pressure gradients, impinging flows and separating flows [121,122].

Realizable  $k$ - $\varepsilon$  model includes new formulation of turbulent viscosity. From a precise equation for the transport of the mean-square vorticity fluctuation, a new transport equation of ' $\varepsilon$ ' has been derived. The term "realizable" refers to a model that satisfied specific mathematical limitations on the Reynolds stresses, in accordance with the physics of turbulent flows.

$$\frac{\partial(\rho k)}{\partial t} + \frac{\partial(\rho k u_j)}{\partial x_j} = \frac{\partial}{\partial x_j} \left[ \left( \mu + \frac{\mu_t}{\sigma_k} \right) \frac{\partial k}{\partial x_j} \right] + G_k + G_b - \rho \varepsilon - Y_M + S_k \quad (7)$$

$$\frac{\partial(\rho\varepsilon)}{\partial t} + \frac{\partial(\rho\varepsilon u_j)}{\partial x_j} = \frac{\partial}{\partial x_j} \left[ \left( \mu + \frac{\mu_t}{\sigma_\varepsilon} \right) \frac{\partial \varepsilon}{\partial x_j} \right] + \rho C_1 S_\varepsilon - \rho C_2 \frac{\varepsilon^2}{k + \sqrt{\nu \varepsilon}} + C_{\varepsilon 1} \frac{\varepsilon}{k} C_{\varepsilon 3} G_b + S_\varepsilon \quad (8)$$

Here,

$$C_1 = \max \left[ 0.43, \frac{\eta}{\eta + 5} \right], \quad \eta = S \frac{k}{\varepsilon}, \quad S = \sqrt{2 S_{ij} S_{ij}} \quad (9)$$

In this model, equation for eddy viscosity is same as standard  $k$ - $\varepsilon$  model but in this value of  $C_\mu$  is not constant. It is computed as,

$$C_\mu = \frac{1}{A_0 + A_s \frac{kU^*}{\varepsilon}} \quad (10)$$

Where,

$$U^* = \sqrt{S_{ij} S_{ij} + \overline{\Omega'_{ij} \Omega'_{ij}}}$$

$$A_0 = 4.04, \quad A_s = \sqrt{6} \cos \phi$$

$$\Omega'_{ij} = \Omega_{ij} - 2\varepsilon_{ijk} \omega_k, \quad \Omega_{ij} = \overline{\Omega_{ij}} - \varepsilon_{ijk} \omega_k$$

$$\phi = \frac{1}{3} \cos^{-1}(\sqrt{6}W), \quad W = \frac{S_{ij} S_{jk} S_{ki}}{\tilde{S}^3}, \quad \tilde{S} = \sqrt{S_{ij} S_{ij}}$$

$$S_{ij} = \frac{1}{2} \left( \frac{\partial u_j}{\partial x_i} + \frac{\partial u_i}{\partial x_j} \right)$$

$\overline{\Omega_{ij}}$  = mean rate of rotation tensor viewed in a rotating reference frame with the angular velocity  $\omega_k$ . The model constants are:  $C_{\varepsilon 1} = 1.44$ ,  $C_{\varepsilon 2} = 1.9$ ,  $\sigma_k = 1.0$ ,  $\sigma_\varepsilon = 1.2$ .

$k$ - $\omega$  model is similar to  $k$ - $\varepsilon$  model, except that it solves for  $\omega$  (omega).  $\omega$  indicates specific rate of kinetic energy dissipation. It is a model with low Reynolds number that can also be used with wall functions. It is more nonlinear and, therefore, more difficult to converge than the  $k$ - $\varepsilon$  model, and it is extremely sensitive to the initial solution guess. The  $k$ - $\omega$  model is applicable in numerous situations when the  $k$ - $\varepsilon$  model is not precise, such as internal flows, flows with severe curvature, separated flows, and jets. Internal flow is exemplified by the flow through a pipe bend [123]. ANSYS's Standard  $k$ - $\omega$  model is derived from Wilcox  $k$ - $\omega$  model [124] with changes for low Reynolds number effects, shear flow spreading and compressibility. The Wilcox model is relevant to wall-bounded flows and free shear flows because it predicts free shear flow spreading rates that are in close agreement with data for far wakes, round, radial, and plane jets and mixing layers. SST (Shear Stress Transport)  $k$ - $\omega$  model, a variant of  $k$ - $\omega$  model, is also accessible in ANSYS Fluent. Standard  $k$ - $\omega$  model is an empirical model based on model transport equations for the  $k$  and  $\omega$ .  $\omega$  commonly known as ratio of  $\varepsilon$  to  $k$  [124]. As the  $k$ - $\omega$  model has been changed throughout time, production terms have been added to both the  $k$  and  $\omega$  equations, thereby enhancing the model's ability to predict free shear flows. This modification improves the model's ability to handle vortexes, and it can also be applied to the viscous sublayer. In addition, it is capable of handling negative pressure gradients and the wall-boundary flow is well resolved if the Reynolds number is low. However, the model's handling is inferior for the freestream [122,125].

Considering above all reviews it is observed that stirrer design parameters such as stirrer shape, stirrer blade angle, stirring speed and stirring time affects mechanical properties of fabricated composites. Blade angles of 30° and 45° and stirring speeds in the range of 300 to 600 rpm is suggested suitable for manufacturing of MMCs by different researchers but still there are chances of porosity and inhomogeneous particle distribution. There is still further need of research in the area of stirrer and its blades design to reduce chances of porosity and improve homogeneous particle distribution. Use of CFD simulation tool and physical simulation will be more suitable approach for stirrer design and shape selection before considering actual manufacturing to reduce cost and save time.

## 6. Al MMCs Applications

Al MMCs are useful in many industrial sectors such as automobile, defense, marine and general engineering due to its suitability to provide combination of properties such as light weight, toughness, high strength to weight ratio, corrosion resistance, wear resistance and easy fabrication. More than 50% of production of MMCs has application in the automotive industry. Important applications mentioned in publications are shown in Fig. 9. Al/SiC composites are widely used in manufacturing of parts such as pistons, calipers, brake rotors, liners, propeller shaft, PCB heat sink, engine cradle and drive shaft. SiC particles are mostly used as reinforcement material in MMCs used in race cars. Some of the Al/Al<sub>2</sub>O<sub>3</sub> composites finds their applications in fabrication of engine blocks, piston rings and connecting rods [126]. Singh et al., [14] provided detailed review on application of MMCs in automobile sector. They reported use of Al/SiC whiskers to fabricate aircraft wing panels and use of Al/Graphite fibers in fabrication of missile and helicopter components. They also reported use of matrix materials such as Al6061-T6, Al6106-T6, Al7075-T651, Al7050-T7451 and various reinforcement materials to fabricate gears having light weight and better mechanical properties to manufacture light weight vehicles. A359/AlN composites were developed for automotive applications and showed improvement in hardness, ultimate tensile strength and yield strength with increase in wt.% of AlN from 5 to 15% [127]. Al/Graphite MMC are useful for manufacturing of cylinder and bearings due to advantage of reduced friction, weight and wear. Al/TiC MMC reduced wear and weight compared to base alloy and is suitable for manufacturing of piston and connecting rod. Al-Si-Zr hybrid MMCs are useful in manufacturing of cutting tools and impellers due to hard structure and high abrasion resistance [128].

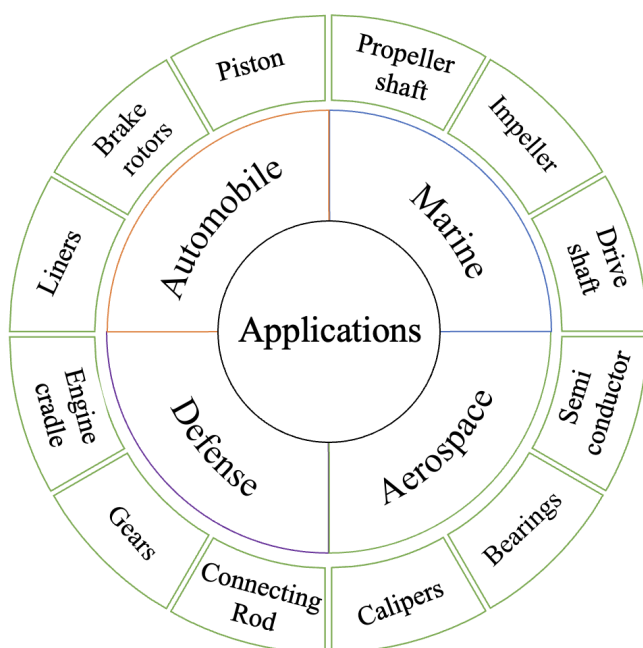


Fig. 9. Al MMCs applications

Sharma et al., [83] fabricated Al-Mg-Si-T6/5% SiC/3% muscovite MMC which showed decrease in wear loss and enhancement of traction strength. They proposed use of this MMC for high strength applications. Kumar et al., [84] developed Al-Mg-Si-T6/5% fly ash/5% B<sub>4</sub>C MMC to suit needs of automotive applications such as high strength and low density. They reported that prepared MMC can be used to fabricate drive shaft of a racing cars. Aigbodion et al., [88] studied microstructure, corrosion and stress analysis of Al-3.7% Cu-1.4% Mg/1.5% rise husk ash nano particles to replace mild steel for the production of impeller. Al7075 reinforced with varying weight percentage of B<sub>4</sub>C and 3 wt.% of BN, improves strength by 22% to that of base alloy. With the addition of B<sub>4</sub>C corrosion rate also decreased. Al7075/B<sub>4</sub>C/BN MMCs are supposed to be used for marine applications. Al6061/10 wt.% B<sub>4</sub>C/3 wt.% Mica hybrid MMC showed best mechanical properties making them suitable for automotive related sheet forming operations. Sahoo et al., [77] focused on manufacturing of self-lubricating composite of Al-SiC-hBN. They successfully fabricated hybrid MMC having 4 wt.% SiC and 5 wt.% hBN which gave max wear resistance and hardness. They mentioned use of this composite for components subjected to wear environment such as bearing. Al6063/5% B<sub>4</sub>C composite suited for use as a steel replacement in nuclear applications. Reinforcement of Al 5xxx series with SiC, B<sub>4</sub>C and Al<sub>2</sub>O<sub>3</sub> are suitable for marine applications, building and construction, automotive and structural applications. MMC fabricated using Al 6xxx series reinforced with SiC, B<sub>4</sub>C and TiB<sub>2</sub> are useful for electronic packaging, marine frames, precision instruments, pipeline and rail rods etc. Al 7xxx series reinforced with SiC, graphite, fly ash and short basalt fiber found their applications on automotive components and large structural members [129]. Other than this, there are many field such as rail transport, building and construction, high temperature applications, electronic packaging, thermal management, electrical transmission and aerospace where needs of MMCs is higher to meet the current market of combination of properties [130].

Some of Al MMCs are utilized in manufacturing of commercial components also by different companies. Ferrotec corporation [131] developed Al/SiC composites and used for semiconductor equipment and inspection parts, display equipment parts, precision equipment parts and heat sinks. CeramTec [132] developed Al MMC having 60 vol.% AlSiMgMn and 40 vol.% Al<sub>2</sub>O<sub>3</sub>. They used composite for manufacturing of engine cylinder sleeves, piston recess walls, brake pad, backing plates, bearings, brake discs, sport goods or heat sinks in electronics. II-VI company [133] developed Al MMCs having base alloy AA360. Reported specific stiffness and thermal stability of developed MMCs are higher than that of stainless steel 303 and Al 6061-T6. They used it for manufacturing of advanced back-end semiconductor processing equipment. Along with these many advantages and applications of Al MMCs, researchers also reported certain obstacles observed such as particle clustering inside matrix, poor wettability, high porosity and higher cost of ceramic particles.



## 7. Conclusions

Metal matrix composites have been developed to meet current market need. Different MMC manufacturing methods, as well as the usage of matrix and reinforcing materials, have been evaluated in order to identify potential improvements in MMC characteristics and quality. The most common matrix materials were Al, Cu, Mg, Si, Fe, Ni, Ti, and their alloys. It is observed that Al and its alloys were mostly used as matrix material due to its easy availability, light weight and low cost. SiC, Al<sub>2</sub>O<sub>3</sub>, and B<sub>4</sub>C were mostly used as reinforcements because they can provide a variety of properties, including high strength, low weight, good wear resistance and corrosion resistance, depending on needs. Selection of reinforcement depends on end application of fabricated MMCs. Hence, selection of suitable reinforcement is most important. List of mostly used reinforcements with their properties and possible bonding mechanism with Al is provided which will be helpful to select suitable reinforcement materials. Further, research can be focused on mixing rare earth materials with different matrix and reinforcement materials to study its effect on properties of fabricated MMCs.

MMCs can be manufactured by varieties of methods. After collecting papers from science direct, it is analyzed that most commonly adopted MMC manufacturing processes are stir casting, powder metallurgy and FSP. Almost 50% of contribution is observed of stir casting process in MMC manufacturing. Stir casting process is reported to be suitable and economical for mass production of MMCs due to low cost. Major limitation of powder metallurgy process is the high cost of metal powder and difficulty in producing uniform density product. Use of FSP is limited due to expensive tooling involved and high frequency usage. Use of stir casting process is mostly reported for manufacturing of Al MMCs due to low melting point of Al and its alloys. Selection of Al as a matrix material by different researchers is due to possibility of achieving combination of properties such as high strength, low weight, better wear resistance, corrosion resistance and high toughness. Several stir casting process parameters that influence the quality of manufactured MMCs need to be optimized. A detailed cause and effect diagram is provided, taking into account all potential variables that could affect the physical characteristics, tribological properties, and porosity of stir cast MMCs.

In recent publications, various wrought and cast Al alloys were explored as matrix materials. Wrought Al alloys reported were AA2024, AA6061, AA6083, AA6351, AA7075 and AA7178. Cast Al alloys reported were LM6, LM7, LM12, LM30, Al-Mg-Si and Al-Cu. It is observed that publications on Al MMCs are mostly focused on parameters such as effect of variation in proportion of different reinforcements to improve the mechanical, thermal and tribological properties. However, limited number of publications have been reported on the effect of stirrer blade design and parameters such as stirrer shape, stirrer dimensions and stirrer position.

The literatures on optimum stirring parameters and their effect on mechanical characteristics and microstructure are re-

viewed. Stirrer design parameters involves stirrer shape, stirrer dimensions, stirrer stages, blade design and blade angles. Stirrer design parameters affects formation of vortex during mixing which in turn affects distribution of reinforcement particles. Particle distribution governs the properties of cast composites. It is reported that stirrer having four blade and 30° or 45° blade angle showed uniform particle distribution inside the melt due to suitable lift forces. Stirring position suggested is 40% from the base. Different stirring speeds in the range of 300 to 600 rpm are recommended. The speed should be chosen so that it does not generate a lot of vortex because that can lead to air entrapment, which increases the chances of porosity formation. The use of an alternate paddle blade and a four blade mixed stirrer resulted in homogenous particle distribution as well.

It is difficult to observe how the particles are dispersed and how the flow behaves during mixing as stir casting process is performed in a closed environment. Some of the methodologies documented in the literature are CFD simulation and physical simulation utilizing a water, glycerol, and graphite mixture. Mostly reported CFD simulation tool is ANSYS Fluent due to easy access of its resources and widespread commercial use. Multiphysics models used for CFD simulation were *k-ε* model and *k-ω* model. It is necessary to assess which of these models best handles the real-time situation. This can be seen as the future scope of this field. In the case of physical simulation, the viscosity of the water-glycerol mixture and the utilization of particles in it are determined by the viscosity of the Al melt and the density difference between the Al melt and the specified reinforcements, respectively. Further research on stirrer design parameters is required to limit the likelihood of porosity formation and achieve homogenous particle distribution. CFD simulation and/or physical simulation will be a better way for stirrer design parameter optimization in order to reduce costs and time.

Al MMCs have made its way into applications in the automotive, defense, aerospace, marine, and general engineering fields thanks to their versatility for providing combinations of properties dependent on needs. Almost half of all MMCs manufactured to date have found use in the automotive industry. Still, commercialization of Al MMCs is challenge. Some of the companies such as Ferrotec, CeramTec and II-VI developed Al/SiC, Al/Al<sub>2</sub>O<sub>3</sub> composites for manufacturing of semiconductor equipment, engine blocks, brake pad and many more.

Major problems reported with the use of stir casting process are lack of homogeneous distribution of particles inside melt, poor wettability and porosity. Wettability improvement methods reported are preheating of reinforcements, addition wetting agents, optimum stirrer design and semi solid stirring. Particle distribution is majorly affected by stirrer geometry. Published stirrer designs are also combined here under one roof which will be helpful for further selection of stirrer geometry and make suitable changes in it. Stirrer design selection considering physics behind it can be well-thought-out as the future area of research in widely adopted stir casting field.

## REFERENCES

- [1] J.D. Selvam, I. Dinaharan, R.S. Rai, Matrix and Reinforcement Materials for Metal Matrix Composites, 2021 Elsevier Ltd.
- [2] M. Haghshenas, Reference Module in Materials Science and Materials Engineering, Metal-Matrix Composites 1-28 (2016). DOI: <https://doi.org/10.1016/b978-0-12-803581-8.03950-3>
- [3] J. Suthar, K.M. Patel, Materials and Manufacturing Processes, Processing issues, machining, and applications of aluminum metal matrix composites **33**, 5, 499-527 (2018). DOI: <https://doi.org/10.1080/10426914.2017.1401713>
- [4] B. Kumar, J.V. Menghani, International Journal of Materials Engineering Innovation, Aluminium-based metal matrix composites by stir casting: A literature review **7**, 1, 1-14 (2016). DOI: <https://doi.org/10.1504/IJMATEI.2016.077310>
- [5] F. Muhammad, S. Jalal, Advances in Materials Science and Engineering, A Comparative Study of the Impact of the Stirrer Design in the Stir Casting Route to Produce Metal Matrix Composites, 2021 (2021). DOI: <https://doi.org/10.1155/2021/4311743>
- [6] P. Samal, P.R. Vundavilli, A. Meher, M.M. Mahapatra, Journal of Manufacturing Processes, Recent progress in aluminum metal matrix composites: A review on processing, Mechanical and Wear Properties **59**, 131-152 (2020). DOI: <https://doi.org/10.1016/j.jmapro.2020.09.010>
- [7] M.Y. Zhou, L.B. Ren, L.L. Fan, Y.W.X. Zhang, T.H. Lu, G.F. Quan, M. Gupta, Journal of Alloys and Compounds, Progress in research on hybrid metal matrix composites, **838**, (2020). DOI: <https://doi.org/10.1016/j.jallcom.2020.155274>
- [8] A. Ramanathan, P.K. Krishnan, R. Muraliraja, Journal of Manufacturing Processes, A review on the production of metal matrix composites through stir casting – Furnace design, properties, challenges, and research opportunities **42**, 213-245 (2019). DOI: <https://doi.org/10.1016/j.jmapro.2019.04.017>
- [9] P. Garg, A. Jamwal, D. Kumar, K.K. Sadasivuni, C.M. Hussain, P. Gupta, Journal of Materials Research and Technology, Advance research progresses in aluminium matrix composites: Manufacturing & Applications **8**, 5, 4924-4939 (2019). DOI: <https://doi.org/10.1016/j.jmrt.2019.06.028>
- [10] M.K. Sahu, R.K. Sahu, Fabrication of Aluminum Matrix Composites by Stir Casting Technique and Stirring Process Parameters Optimization, in: T. Vijayaram, Advanced Casting Technologies 2018, IntechOpen (2018). DOI: <https://doi.org/10.5772/intechopen.73485>
- [11] A.M. Razzaq, D.L.A. Abdul Majid, M.R. Ishak, M.B. Uday, IOP Conference Series: Materials Science and Engineering, A Brief Research Review for Improvement Methods the Wettability between Ceramic Reinforcement Particulate and Aluminium Matrix Composites **203**, 1 (2017). DOI: <https://doi.org/10.1088/1757-899X/203/1/012002>
- [12] M. Malaki, A.F. Tehrani, B. Niroumand, M. Gupta, Metals, Wettability in metal matrix composites **11**, 7, 1-24 (2021). DOI: <https://doi.org/10.3390/met11071034>
- [13] T. Yamamoto, A. Suzuki, S.V. Komarov, Y. Ishiwata, Journal of Materials Processing Technology, Investigation of impeller design and flow structures in mechanical stirring of molten aluminum **261**, 164-172 (2018). DOI: <https://doi.org/10.1016/j.jmatprotec.2018.06.012>
- [14] H. Singh, G. Singh, H. Kumar, V. Aggarwal, Materials Today: Proceedings, A review on metal matrix composite for automobile applications **43**, 320-325 (2020). DOI: <https://doi.org/10.1016/j.matpr.2020.11.670>
- [15] H. Zhou, P. Yao, T. Gong, Y. Xiao, Z. Zhang, L. Zhao, K. Fan, M. Deng, Tribology International, Effects of ZrO<sub>2</sub> crystal structure on the tribological properties of copper metal matrix composites **138**, May, 380-391 (2019). DOI: <https://doi.org/10.1016/j.triboint.2019.06.005>
- [16] A. Jamwal, P. Mittal, R. Agrawal, S. Gupta, D. Kumar, K. Sadasivuni, P. Gupta, Journal of Composite Materials, Towards sustainable copper matrix composites: Manufacturing routes with structural, mechanical, electrical and corrosion behaviour, **54**, 19, 2635-2649 (2020). DOI: <https://doi.org/10.1177/0021998319900655>
- [17] A. Dey, K.M. Pandey, Reviews on Advanced Materials Science, Magnesium metal matrix composites-a review **42**, 1, 58-67 (2015).
- [18] D. Dash, S. Samanta, R.N. Rai, IOP Conference Series: Materials Science and Engineering, Study on Fabrication of Magnesium based Metal Matrix Composites and its improvement in Mechanical and Tribological Properties – A Review **377**, 1, (2018). DOI: <https://doi.org/10.1088/1757-899X/377/1/012133>
- [19] M.D. Hayat, H. Singh, Z. He, P. Cao, Composites Part A: Applied Science and Manufacturing, Titanium metal matrix composites: An overview, 121, March, 418-438 (2019). DOI: <https://doi.org/10.1016/j.compositesa.2019.04.005>
- [20] S. Luo, T. Song, B. Liu, J. Tian, M. Qian, Advanced Engineering Materials, Recent Advances in the Design and Fabrication of Strong and Ductile (Tensile) Titanium Metal Matrix Composites **21**, 7, 1-13 (2019). DOI: <https://doi.org/10.1002/adem.201801331>
- [21] B.K. Kumar, M.G. Ananthaprasad, K. GopalaKrishna, Indian Journal of Science and Technology, A review on mechanical and tribological behaviors of nickel matrix composites **9**, 2 (2016). DOI: <https://doi.org/10.17485/ijst/2016/v9i2/82868>
- [22] S. Simões, F. Viana, M.A. L. Reis, M.F. Vieira, Metals, Aluminum and nickel matrix composites reinforced by CNTs: Dispersion/mixture by ultrasonication, **7**, 7 (2017). DOI: <https://doi.org/10.3390/met7070279>
- [23] E. E. Feldshtein, L. N. Dyachkova, Wear, Wear minimization for highly loaded iron-based MMCs due to the formation of spongy-capillary texture on the friction surface **444-445**, 20316 (2020). DOI: <https://doi.org/10.1016/j.wear.2019.203161>
- [24] Z. Wang, M. Tan, J. Wang, J. Zeng, F. Zhao, X. Xiao, S. Xu, B. Liu, L. Gong, Q. Sui, R. Zhang, B. Han, J. Liu, Journal of Alloys and Compounds, Core-shell structural iron based metal matrix composite powder for laser cladding **878**, 160127 (2021). DOI: <https://doi.org/10.1016/j.jallcom.2021.160127>
- [25] Y. Fang, M. Kim, Y. Zhang, Z. Duan, Q. Yuan, J. Suhr, Journal of Manufacturing Processes, Particulate-reinforced iron-based metal matrix composites fabricated by selective laser melting: A systematic review, 74, December, 592-639 (2022). DOI: <https://doi.org/10.1016/j.jmapro.2021.12.018>

- [26] J. Wiecek, B. Oleksiak, J. Łabaj, B. Węcki, M. Mańka, *Archives of Metallurgy and Materials, Silver matrix composites – Structure and properties* **61**, 1, 323-328 (2016).  
DOI: <https://doi.org/10.1515/amm-2016-0060>
- [27] C. Nikhilesh, C. Krishan, *Metal Matrix Composites*, 2013 Springer, New York.
- [28] K.U. Kainer, *Metal Matrix Composites Custom-made Materials for Automotive and Aerospace Engineering*, 2006 Wiley-VCH, Weinheim.
- [29] K. Suryanarayanan, R. Praveen, S. Raghuraman, *International Journal of Innovative Research in Science, Engineering and Technology, Silicon Carbide Reinforced Aluminium Metal Matrix Composites for Aerospace Applications: A Literature Review* **2**, 11, 6336-6344 (2007).
- [30] V.S. Mann, O.P. Pandey, *Wear, Influence of natural beach mineral corundum on the wear characteristics of LM30 aluminium alloy composites*, 477, March, (2021).  
DOI: <https://doi.org/10.1016/j.wear.2021.203801>
- [31] A. Kareem, J.A. Qudeiri, A. Abdudeen, T. Ahammed, A. Ziout, *Materials, A review on AA 6061 metal matrix composites produced by stir casting* **14**, 1 (2021).  
DOI: <https://doi.org/10.3390/ma14010175>
- [32] L. Zhang, G. Shi, X. Kun, H. Wu, Q. Li, J. Wu, Z. Wang, *Journal of Materials Research and Technology, Phase transformation and mechanical properties of B4C/Al composites* **9**, 2, 2116-2126 (2020).  
DOI: <https://doi.org/10.1016/j.jmrt.2019.12.042>
- [33] A.R. Kennedy, D.P. Weston, M.I. Jones, *Materials Science & Engineering A, Reaction in Al-TiC metal matrix composites* **316**, 1-2, 32-38 (2001).  
DOI: [https://doi.org/10.1016/S0921-5093\(01\)01228-X](https://doi.org/10.1016/S0921-5093(01)01228-X)
- [34] C. Mao, X. Sun, Q. Liang, J. Yang, J. Du, *Rare Metals, Interfacial reaction process of the hot-pressed WC/2024Al composite* **32**, 397-401 (2013). DOI: <https://doi.org/10.1007/s12598-013-0116-z>
- [35] B. Tang, Y. Tan, T. Xu, Z. Sun, X. Li, *Coatings, Effects of TiB2 particles content on Microstructure, Mechanical Properties and Tribological Properties of Ni-Based Composite Coatings Reinforced with TiB2*, **10**, 9 (2020).  
DOI: <https://doi.org/10.3390/coatings10090813>
- [36] K.L. Tee, L. Lu, M.O. Lai, *Journal of Materials Processing Technology, In situ processing of Al-TiB2 composite by the stir-casting technique* **89-90**, 513-519 (1999).  
DOI: [https://doi.org/10.1016/S0924-0136\(99\)00038-2](https://doi.org/10.1016/S0924-0136(99)00038-2)
- [37] P.S. Shreyas, B.P. Mahesh, S. Rajanna, N. Rajesh, *Materials Today: Proceedings, Evaluating the tribological properties of aluminium based hybrid composites reinforced with Al2O3 & ZrO2 nano particles* **5**, 429-433 (2020).  
DOI: <https://doi.org/10.1016/j.matpr.2020.12.1012>
- [38] M. Rajasekar, U.M. Faizal, S. Sudhagar, P. Vijayakumar, *Materials Today: Proceedings, Influence of heat treatment on tribological behavior of Al/ZrO2/fly ash hybrid composite* **45**, 774-779 (2021).  
DOI: <https://doi.org/10.1016/j.matpr.2020.02.805>
- [39] V. Khalili, A. Heidarzadeh, S. Moslemi, L. Fathyunes, *Journal of Materials Research and Technology, Production of Al6061 matrix composites with ZrO2 ceramic reinforcement using a low-cost stir casting technique: Microstructure, mechanical properties, and electrochemical behavior* **9**, 6, 15072-15086 (2020).  
DOI: <https://doi.org/10.1016/j.jmrt.2020.10.095>
- [40] <https://www.azonano.com/article.aspx?ArticleID=3351>, accessed: 25.11.2022
- [41] L. Fan, L. Yang, D. Zhao, L. Ma, C. He, F. He, C. Shi, J. Sha, N. Zhao, *Materials, Balancing Strength and Ductility in Al Matrix Composites Reinforced by Few-Layered MoS2 through In-Situ Formation of Interfacial Al12Mo* **14**, 13 (2021).  
DOI: <https://doi.org/10.3390/ma14133561>
- [42] N. Kumar, R.K. Gautam, S. Mohan, *Materials and Design, In-situ development of ZrB2 particles and their effect on microstructure and mechanical properties of AA5052 metal-matrix composites* **80**, 129-136 (2015).  
DOI: <https://doi.org/10.1016/j.matdes.2015.05.020>
- [43] I. Dinaharan, *Liquid metallurgy processing of intermetallic matrix composites*, in: R. Mitra, *Intermetallic Matrix Composites Properties and Applications*, Woodhead Publishing 2017.
- [44] J.D.R. Selvam, I. Dinaharan, *Engineering Science and Technology, an International Journal, In situ formation of ZrB2 particulates and their influence on microstructure and tensile behavior of AA7075 aluminum matrix composites* **20**, 1, 187-196 (2017).  
DOI: <https://doi.org/10.1016/j.jestech.2016.09.006>
- [45] L. Ci, Z. Ryu, N.Y. Jin-phillipp, M. Ruhle, *Acta Materialia, Investigation of the interfacial reaction between multi-walled carbon nanotubes and aluminum* **54**, 5367-5375 (2006).  
DOI: <https://doi.org/10.1016/j.actamat.2006.06.031>
- [46] J. Li, X. Zhang, L. Geng, *Composites Part A, Effect of heat treatment on interfacial bonding and strengthening efficiency of graphene in GNP/Al composites* **121**, April, 487-498 (2019).  
DOI: <https://doi.org/10.1016/j.compositesa.2019.04.010>
- [47] J.B. Rao, D.V. Rao, I.N. Murthy, N. Bhargava, *Journal of Composite Materials, Mechanical properties and corrosion behaviour of fly ash particles reinforced AA 2024 composites* **46**, 12, 1393-1404 (2012). DOI: <https://doi.org/10.1177/0021998311419876>
- [48] S. Kumar, R. Singh, M.S.J. Hashmi, *Advances in Materials and Processing Technologies, Metal matrix composite: a methodological review* **6**, 1, 13-24 (2020).  
DOI: <https://doi.org/10.1080/2374068X.2019.1682296>
- [49] M. Meignanamoorthy, M. Ravichandran, *Mechanics and Mechanical Engineering, Synthesis of metal matrix composites via powder metallurgy route: A review* **22**, 1, 65-75 (2018).  
DOI: <https://doi.org/10.2478/mme-2018-0007>
- [50] G.A.W. Sweet, B.W. Williams, A. Taylor, R.L. Hexemer, I.W. Donaldson, D.P. Bishop, *Journal of Materials Processing Technology, A microstructural and mechanical property investigation of a hot upset forged 2xxx series aluminum powder metallurgy alloy reinforced with AlN*, 284, May, (2020).  
DOI: <https://doi.org/10.1016/j.jmatprotec.2020.116742>
- [51] S. Sun, N. Deng, H. Zhang, L. He, H. Zhou, B. Han, K. Gao, X. Wang, *Journal of Materials Research and Technology, Microstructure and mechanical properties of AZ31 magnesium alloy reinforced with novel sub-micron vanadium particles by powder metallurgy* **15**, 1789-1800 (2021).  
DOI: <https://doi.org/10.1016/j.jmrt.2021.09.015>

- [52] N. Gangil, A.N. Siddiquee, S. Maheshwari, *Journal of Alloys and Compounds*, Aluminium based in-situ composite fabrication through friction stir processing: A review **715**, 91-104 (2017). DOI: <https://doi.org/10.1016/j.jallcom.2017.04.309>
- [53] I. Dinaharan, N. Murugan, E.T. Akinlabi, *Friction Stir Processing Route for Metallic Matrix Composite Production*, 2021 Elsevier Ltd.,
- [54] N. Bharat, P.S.C. Bose, *Materials Today: Proceedings*, An overview on the effect of reinforcement and wear behaviour of metal matrix composites **46**, 707-713 (2021). DOI: <https://doi.org/10.1016/j.matpr.2020.12.084>
- [55] M. Narimani, B. Lotfi, Z. Sadeghian, *Materials Science and Engineering A*, Investigating the microstructure and mechanical properties of Al-TiB<sub>2</sub> composite fabricated by Friction Stir Processing (FSP) **673**, 436-442 (2016). DOI: <https://doi.org/10.1016/j.msea.2016.07.086>
- [56] A. Evans, C. Marchi, A. Mortensen, *Metal Matrix Composites in Industry: An Introduction and a Survey*, 2003 Kluwer Academic Publishers.
- [57] Y. Chen, Y. Huang, L. Han, D. Liu, L. Luo, C. Li, C. Liu, Z. Wang, *Journal of Materials Research and Technology*, High-strength vacuum diffusion bonding of Cu-plated, sandblasted W and Cu-CrZr alloy, **15**, November-December, 6260-6271 (2021). DOI: <https://doi.org/10.1016/j.jmrt.2021.11.0691>
- [58] <https://www.phase-trans.msm.cam.ac.uk/2005/Amir/bond.html>, accessed: 28.11.2022
- [59] R. Etemadi, B. Wang, K.M. Pillai, B. Niroumand, E. Omrani, P. Rohatgi, *Materials and Manufacturing Processes*, Pressure infiltration processes to synthesize metal matrix composites – A review of metal matrix composites, the technology and process simulation **33**, 12, 1261-1290 (2018). DOI: <https://doi.org/10.1080/10426914.2017.1328122>
- [60] A.M.S-De-la-muela, L.E.G. Cambronero, J.M. Ruiz-Román, *Metals*, Molten metal infiltration methods to process metal matrix syntactic foams **10**, 1, (2020). DOI: <https://doi.org/10.3390/met10010149>
- [61] M. Yamamoto, Y. Nishimura, M. Hayashida, *Journal of Alloys and Compounds*, Influence of Al particles as infiltration promoters on the interfacial reaction and mechanical property of a continuous SiC fiber/AZ91 composite fabricated by a low-pressure infiltration method, **887**, (2021). DOI: <https://doi.org/10.1016/j.jallcom.2021.161461>
- [62] N. Bouzegzi, D. Miroud, F. Ahnia, G. Alcalá, F. Perez, K. Khenfer, M. Tata, S. Mato, *Journal of Alloys and Compounds*, Microstructural and electrochemical study of a brazed WC based metal matrix composite obtained by infiltration process **759**, 22-31 (2018). DOI: <https://doi.org/10.1016/j.jallcom.2018.05.141>
- [63] A. Sankhla, K.M. Patel, *Advances in Materials and Processing Technologies*, Metal Matrix Composites Fabricated by Stir Casting Process – A Review **8**, 2, 1270-1291 (2021). DOI: <https://doi.org/10.1080/2374068X.2020.1855404>
- [64] G. Nageswaran, S. Natarajan, K.R. Ramkumar, *Journal of Alloys and Compounds*, Synthesis, structural characterization, mechanical and wear behaviour of Cu-TiO<sub>2</sub>-Gr hybrid composite through stir casting technique **768**, 733-741 (2018). DOI: <https://doi.org/10.1016/j.jallcom.2018.07.288>
- [65] L. Singh, B. Singh, K.K. Saxena, *Advances in Materials and Processing Technologies*, Manufacturing techniques for metal matrix composites (MMC): An overview **6**, 2, 224-240 (2020). DOI: <https://doi.org/10.1080/2374068X.2020.1729603>
- [66] M. Dhanashekar, V.S. Senthil Kumar, *Procedia Engineering*, Squeeze casting of aluminium metal matrix composites – An overview **97**, 412-420 (2014). DOI: <https://doi.org/10.1016/j.proeng.2014.12.265>
- [67] N.S. Kumar, *Materials Today: Proceedings*, Fabrication and characterization of Al7075 / RHA /Mica composite by squeeze casting **37**, Part 2, 750-753 (2020). DOI: <https://doi.org/10.1016/j.matpr.2020.05.769>
- [68] S.D. Kumar, M. Ravichandran, A. Jeevika, B. Stalin, C. Kailasanathan, A. Karthick, *Ceramics International*, Effect of ZrB<sub>2</sub> on microstructural, mechanical and corrosion behaviour of aluminium (AA7178) alloy matrix composite prepared by the stir casting route **47**, 9, 12951-12962 (2021). DOI: <https://doi.org/10.1016/j.ceramint.2021.01.158>
- [69] A. Alizadeh, A. Khayami, M. Karamouz, M. Hajizamani, *Ceramics International*, Mechanical properties and wear behavior of Al5083 matrix composites reinforced with high amounts of SiC particles fabricated by combined stir casting and squeeze casting: A comparative study **48**, 1, 179-189 (2022). DOI: <https://doi.org/10.1016/j.ceramint.2021.09.093>
- [70] H.I. Akbar, E. Surojo, D. Ariawan, A.R. Prabowo, F. Imanullah, *Heliyon*, Fabrication of AA6061-sea sand composite and analysis of its properties **7**, 8 (2021). DOI: <https://doi.org/10.1016/j.heliyon.2021.e07770>
- [71] A.A. Adediran, A.A. Akinwande, O.A. Balogun, O.S. Adesina, A. Olayanju, T. Mojisola, *Scientific African*, Evaluation of the properties of Al-6061 alloy reinforced with particulate waste glass, **12** (2021). DOI: <https://doi.org/10.1016/j.sciaf.2021.e00812>
- [72] R. Farajollahi, H.J. Aval, R. Jamaati, *Journal of Alloys and Compounds*, Effects of Ni on the microstructure, mechanical and tribological properties of AA2024-Al<sub>3</sub>NiCu composite fabricated by stir casting process, **887** (2021). DOI: <https://doi.org/10.1016/j.jallcom.2021.161433>
- [73] R. Balachandhar, R. Balasundaram, M. Ravichandran, *Journal of Magnesium and Alloys*, Analysis of surface roughness of rock dust reinforced AA6061-Mg matrix composite in turning **9**, 5, 1669-1676 (2021). DOI: <https://doi.org/10.1016/j.jma.2021.03.035>
- [74] K.O. Babaremu, O.O. Joseph, E.T. Akinlabi, T.C. Jen, O.P. Oladijo, *Heliyon*, Morphological investigation and mechanical behaviour of agrowaste reinforced aluminium alloy 8011 for service life improvement **6**, 11 (2020). DOI: <https://doi.org/10.1016/j.heliyon.2020.e05506>
- [75] J. Zhu, W. Jiang, G. Li, F. Guan, Y. Yu, Z. Fan, *Journal of Materials Processing Technology*, Microstructure and mechanical properties of SiCnp/Al6082 aluminum matrix composites prepared by squeeze casting combined with stir casting, **283**, January, (2020). DOI: <https://doi.org/10.1016/j.jmatprotec.2020.116699>
- [76] V. Mohanavel, K.S.A. Ali, S. Prasath, T. Sathish, M. Ravichandran, *Journal of Materials Research and Technology*, Microstructural

- and tribological characteristics of AA6351/Si<sub>3</sub>N<sub>4</sub> composites manufactured by stir casting **9**, 6, 14662-14672 (2020).  
DOI: <https://doi.org/10.1016/j.jmrt.2020.09.128>
- [77] S. Sahoo, S. Samal, B. Bhoi, *Materials Today Communications*, Fabrication and characterization of novel Al-SiC-hBN self-lubricating hybrid composites, **25**, June, (2020).  
DOI: <https://doi.org/10.1016/j.mtcomm.2020.101402>
- [78] S. Gudipudi, S. Nagamuthu, K.S. Subbian, S.P.R. Chilakalapalli, *Engineering Science and Technology, an International Journal*, Enhanced mechanical properties of AA6061-B4C composites developed by a novel ultra-sonic assisted stir casting **23**, 5, 1233-1243 (2020).  
DOI: <https://doi.org/10.1016/j.jestch.2020.01.010>
- [79] M. Shayan, B. Eghbali, B. Niroumand, *Materials Science and Engineering A*, Synthesis of AA2024-(SiO<sub>2</sub>np+TiO<sub>2</sub>np) hybrid nanocomposite via stir casting process, **756**, February, 484-491 (2019). DOI: <https://doi.org/10.1016/j.msea.2019.04.089>
- [80] B. Subramaniam, B. Natarajan, B. Kaliyaperumal, S.J.S. Chelladurai, *Materials Research Express*, Wear behaviour of aluminium 7075 – Boron carbide – coconut shell fly ash reinforced hybrid metal matrix composites **6**, 10, 449-456 (2019).  
DOI: <https://doi.org/10.1088/2053-1591/ab4052>
- [81] J.D.R. Selvam, I. Dinaharan, S.V. Philip, P.M. Mashinini, *Journal of Alloys and Compounds*, Microstructure and mechanical characterization of in situ synthesized AA6061/(TiB<sub>2</sub>+Al<sub>2</sub>O<sub>3</sub>) hybrid aluminum matrix composites **740**, 529-535 (2018).  
DOI: <https://doi.org/10.1016/j.jallcom.2018.01.016>
- [82] M.E. Turan, F. Aydin, Y. Sun, H. Zengin, Y. Akinay, *Tribology International*, Wear resistance and tribological properties of GNPs and MWCNT reinforced AlSi18CuNiMg alloys produced by stir casting, **164**, April, (2021).  
DOI: <https://doi.org/10.1016/j.triboint.2021.107201>
- [83] S. Sharma, J. Singh, M. Gupta, M. Mia, S. Dwivedi, A. Saxena, S. Chattopadhyaya, R. Singh, D.Y. Pimenov, M. Korkmaz, *Journal of Materials Research and Technology*, Investigation on mechanical, tribological and microstructural properties of Al-Mg-Si-T6/SiC/muscovite-hybrid metal-matrix composites for high strength applications **12**, 1564-1581 (2021).  
DOI: <https://doi.org/10.1016/j.jmrt.2021.03.095>
- [84] M.S. Kumar, M. Vasumathi, S.R. Begum, S.M. Luminita, S. Vlase, C.I. Pruncu, *Journal of Materials Research and Technology*, Influence of B4C and industrial waste fly ash reinforcement particles on the micro structural characteristics and mechanical behavior of aluminium (Al-Mg-Si-T6) hybrid metal matrix composite **15**, 1201-1216 (2021).  
DOI: <https://doi.org/10.1016/j.jmrt.2021.08.149>
- [85] G.B. Rao, P.K. Bannaravuri, R. Raja, K.C. Apparao, P.S. Rao, T.S. Rao, A.K. Birru, R.M.R. Prince, *International Journal of Lightweight Materials and Manufacture*, Impact on the microstructure and mechanical properties of Al-4.5Cu alloy by the addition of MoS<sub>2</sub> **4**, 3, 281-289 (2021).  
DOI: <https://doi.org/10.1016/j.ijlmm.2021.01.001>
- [86] T. Wang, X. Zuo, Y. Zhou, J. Tian, S. Ran, *Journal of Materials Research and Technology*, High strength and high ductility nano-Ni-Al<sub>2</sub>O<sub>3</sub>/A356 composites fabricated with nickel-plating and equal channel angle semi-solid extrusion (ECASE), **13**, 1615-1627 (2021).  
DOI: <https://doi.org/10.1016/j.jmrt.2021.05.083>
- [87] Q. Hu, W. Guo, P. Xiao, J. Yao, *Physica B: Condensed Matter*, First-principles investigation of mechanical, electronic, dynamical, and thermodynamic properties of Al<sub>3</sub>BC, **616**, March, (2021).  
DOI: <https://doi.org/10.1016/j.physb.2021.413127>
- [88] V.S. Aigbodion, P.O. Ozor, M.N. Eke, C.U. Nwoji, *Chemical Data Collections*, Explicit microstructure, corrosion, and stress analysis of value-added Al-3.7%Cu-1.4%Mg/1.5% rice husk ash nanoparticles for pump impeller application, **33**, (2021).  
DOI: <https://doi.org/10.1016/j.cdc.2021.100675>
- [89] S. Singh, K. Pal, *Ceramics International*, Investigation on microstructural, mechanical and damping properties of SiC/TiO<sub>2</sub>, SiC/Li<sub>4</sub>Ti<sub>5</sub>O<sub>12</sub> reinforced Al matrix **47**, 10, 14809-14820 (2021).  
DOI: <https://doi.org/10.1016/j.ceramint.2020.10.068>
- [90] K. Velavan, K. Palanikumar, E. Natarajan, W.H. Lim, *Journal of Materials Research and Technology*, Implications on the influence of mica on the mechanical properties of cast hybrid (Al+10%B4C+Mica) metal matrix composite **10**, 99-109 (2021).  
DOI: <https://doi.org/10.1016/j.jmrt.2020.12.004>
- [91] P. Zhang, W. Zhang, Y. Du, Y. Wang, *Journal of Manufacturing Processes*, High-performance Al-1.5 wt% Si-Al<sub>2</sub>O<sub>3</sub> composite by vortex-free high-speed stir casting, **56**, December, 1126-1135 (2020). DOI: <https://doi.org/10.1016/j.jmapro.2020.06.016>
- [92] W.Y. Zhang, Y.H. Du, P. Zhang, *Journal of Alloys and Compounds*, Vortex-free stir casting of Al-1.5 wt% Si-SiC composite **787**, 206-215 (2019).  
DOI: <https://doi.org/10.1016/j.jallcom.2019.02.099>
- [93] N. Ramadoss, K. Pazhanivel, G. Anbuechezhiyan, *Journal of Materials Research and Technology*, Synthesis of B4C and BN reinforced Al7075 hybrid composites using stir casting method **9**, 3, 6297-6304 (2020).  
DOI: <https://doi.org/10.1016/j.jmrt.2020.03.043>
- [94] J.V. Christy, R. Arunachalam, A.H.I. Mourad, P.K. Krishnan, S. Piya, M. Al-Maharbi, *Journal of Manufacturing Processes*, Processing, Properties, and Microstructure of Recycled Aluminum Alloy Composites Produced Through an Optimized Stir and Squeeze Casting Processes, **59**, December, 287-301 (2020).  
DOI: <https://doi.org/10.1016/j.jmapro.2020.09.067>
- [95] G. Karthikeyan, G. Elatharasan, S. Thulasi, P. Vijayalakshmi, *Materials Today: Proceedings*, Tensile, compressive and heat transfer analysis of ZrO<sub>2</sub> reinforced aluminum LM6 alloy metal matrix composites **37**, Part 2, 303-309 (2020).  
DOI: <https://doi.org/10.1016/j.matpr.2020.05.270>
- [96] M.H. Faisal, V.Sreekumar, N.M. Nidhiry, *Materials Today: Proceedings*, Comparison of mechanical and wearing properties between LM6, LM6/B4C and LM6/B4C/Gr aluminium metal matrix composites **43**, 3916-3921 (2020).  
DOI: <https://doi.org/10.1016/j.matpr.2021.01.340>
- [97] J. Xue, W. Wu, J. Ma, H. Huang, Z. Zhao, *Materials Science and Engineering A*, Study on the effect of CeO<sub>2</sub> for fabricating in-situ TiB<sub>2</sub>/A356 composites with improved mechanical properties, **786**, December, (2020).  
DOI: <https://doi.org/10.1016/j.msea.2020.139416>

- [98] S.L. Pramod, Ravikirana, A.K.P. Rao, B.S. Murty, S.R. Bakshi, *Materials Science and Engineering A*, Microstructure and mechanical properties of as-cast and T6 treated Sc modified A356-5TiB2 in-situ composite, 739, October, 383-394 (2019). DOI: <https://doi.org/10.1016/j.msea.2018.10.080>
- [99] S. Ma, X. Wang, *Materials Science and Engineering A*, Mechanical properties and fracture of in-situ Al3Ti particulate reinforced A356 composites, 754, January, 46-56 (2019). DOI: <https://doi.org/10.1016/j.msea.2019.03.044>
- [100] P.K. Krishnan, J.V. Christy, R. Arunachalam, A-H. I. Mourad, R. Murliraja, M.Al-Maharbi, V. Murli, M.M. Chandra, *Journal of Alloys and Compounds*, Production of aluminum alloy-based metal matrix composites using scrap aluminum alloy and waste materials: Influence on microstructure and mechanical properties, 784, 1047-1061 (2019). DOI: <https://doi.org/10.1016/j.jallcom.2019.01.115>
- [101] A.H. Idrisi, A.H.I. Mourad, *Journal of Alloys and Compounds*, Conventional stir casting versus ultrasonic assisted stir casting process: Mechanical and physical characteristics of AMCs **805**, 502-508 (2019). DOI: <https://doi.org/10.1016/j.jallcom.2019.07.076>
- [102] J. Suthar, K. Patel, *Heliyon*, Identification, screening and optimization of significant parameters for stir cast hybrid aluminium metal matrix composite **4**, 12, (2018). DOI: <https://doi.org/10.1016/j.heliyon.2018.e00988>
- [103] V.R. Mehta, M.P. Sutaria, *Metals and Materials International*, Investigation on the Effect of Stirring Process Parameters on the Dispersion of SiC Particles Inside Melting Crucible **27**, 8, 2989-3002 (2021). DOI: <https://doi.org/10.1007/s12540-020-00612-0>
- [104] M.S. Kumar, S.R. Begum, C.I. Pruncu, M.S. Asl, *Journal of Alloys and Compounds*, Role of homogeneous distribution of SiC reinforcement on the characteristics of stir casted Al-SiC composites, 869 (2021). DOI: <https://doi.org/10.1016/j.jallcom.2021.159250>
- [105] P.K. Krishnan, R. Arunachalam, A. Husain, M. Al-Maharbi, *Journal of Manufacturing Science and Engineering, Transactions of the ASME*, Studies on the influence of stirrer blade design on the microstructure and mechanical properties of a novel aluminum metal matrix composite **143**, 2 (2021). DOI: <https://doi.org/10.1115/1.4048266>
- [106] A. Kumar, R.S. Rana, R. Purohit, *Advances in Materials and Processing Technologies*, Effect of stirrer design on microstructure of MWCNT and Al alloy by stir casting process **6**, 2, 372-379 (2020). DOI: <https://doi.org/10.1080/2374068X.2020.1731156>
- [107] T. Tamilanban, T.S. Ravikumar, S. Kanthasamy, *IOP Conference Series: Materials Science and Engineering*, Influence of stirrer blade design on stir casting of Al Mg Cu/12% SiC composite **988**, 1, (2020). DOI: <https://doi.org/10.1088/1757-899X/988/1/012062>
- [108] M.S. Kumar, C.I. Pruncu, P. Harikrishnan, S.R. Begum, M. Vasumathi, *Silicon*, Experimental Investigation of In-homogeneity in Particle Distribution During the Processing of Metal Matrix Composites **14**, 629-641 (2022). DOI: <https://doi.org/10.1007/s12633-020-00886-4>
- [109] J.J. Moses, S.J. Sekhar, *Transactions of the Indian Institute of Metals*, Investigation on the Tensile Strength and Microhardness of AA6061/TiC Composites by Stir Casting **70**, 4, 1035-1046 (2017). DOI: <https://doi.org/10.1007/s12666-016-0891-y>
- [110] J. J. Moses, I. Dinaharan, S. J. Sekhar, *Transactions of Nonferrous Metals Society of China (English Edition)*, Prediction of influence of process parameters on tensile strength of AA6061/TiC aluminum matrix composites produced using stir casting **26**, 6, 1498-1511 (2016). DOI: [https://doi.org/10.1016/S1003-6326\(16\)64256-5](https://doi.org/10.1016/S1003-6326(16)64256-5)
- [111] R.T. Bui, R. Ouellet, D. Kocaefe, *Metallurgical and Materials Transactions B*, A two-phase flow model of the stirring of Al-SiC composite melt **25**, 4, 607-618 (1994). DOI: <https://doi.org/10.1007/BF02650081>
- [112] P.K. Rohatgi, J. Sobczak, R. Asthana, J.K. Kim, *Materials Science and Engineering A*, Inhomogeneities in silicon carbide distribution in stirred liquids – A water model study for synthesis of composites **252**, 1, 98-108 (1998). DOI: [https://doi.org/10.1016/S0921-5093\(98\)00651-0](https://doi.org/10.1016/S0921-5093(98)00651-0)
- [113] P.K. Biswas, S.C. Dev, K.M. Godiwalla, C.S. Sivaramakrishnan, *Materials and Design*, Effect of some design parameters on the suspension characteristics of a mechanically agitated sand-water slurry system **20**, 5, 253-265 (1999). DOI: [https://doi.org/10.1016/s0261-3069\(98\)00036-3](https://doi.org/10.1016/s0261-3069(98)00036-3)
- [114] S. Naher, D. Brabazon, L. Looney, *Journal of Materials Processing Technology*, Simulation of the stir casting process **143-144**, 1, 567-571 (2003). DOI: [https://doi.org/10.1016/S0924-0136\(03\)00368-6](https://doi.org/10.1016/S0924-0136(03)00368-6)
- [115] S. Naher, D. Brabazon, L. Looney, *Composites Part A: Applied Science and Manufacturing*, Computational and experimental analysis of particulate distribution during Al-SiC MMC fabrication **38**, 3, 719-729 (2007). DOI: <https://doi.org/10.1016/j.compositesa.2006.09.009>
- [116] H. Su, W. Gao, H. Zhang, H. Liu, J. Lu, Z. Lu, *Journal of Manufacturing Science and Engineering, Transactions of the ASME*, Optimization of stirring parameters through numerical simulation for the preparation of aluminum matrix composite by stir casting process **132**, 6, 0610071-0610077 (2010). DOI: <https://doi.org/10.1115/1.4002851>
- [117] M.V.S.P. Kumar, M.V.S. Babu, V. Ramana, *Journal of Engineering Research and Applications*, Simulation of Stir Casting Process Using Computational Fluid Dynamics **5**, 8, 132-135 (2015).
- [118] K.V. Prasad, K.R. Jayadevan, *Procedia Technology*, Simulation of Stirring in Stir Casting **24**, 356-363 (2016). DOI: <https://doi.org/10.1016/j.protcy.2016.05.048>
- [119] K. Rajendra, M.V.S Babu, P. Srinivas, *IOP Conference Series: Materials Science and Engineering*, Stir Casting Process Simulation by Computational Fluid Dynamics for uniform Nano particles distribution in Al Semi Solid Metal **377**, 1 (2018). DOI: <https://doi.org/10.1088/1757-899X/377/1/012191>
- [120] M. Foukrach, M. Bouzit, H. Ameer, Y. Kamla, *Chinese Journal of Mechanical Engineering (English Edition)*, Effect of Agitator's Types on the Hydrodynamic Flow in an Agitated Tank **33**, 1 (2020). DOI: <https://doi.org/10.1186/s10033-020-00454-2>

- [121] W.P. Jones, B.E. Launder, *International Journal of Heat and Mass Transfer*, The prediction of laminarization with a two-equation model of turbulence **15**, 301-314 (1972).  
DOI: [https://doi.org/10.1016/0017-9310\(72\)90076-2](https://doi.org/10.1016/0017-9310(72)90076-2)
- [122] S.P. Ruiz, Study of flow fields in mixing tanks with particles using CFD, PHD thesis, LUND University, June 2021.
- [123] <https://www.comsol.com/blogs/which-turbulence-model-should-choose-cfd-application/>, accessed: 10.07.2022
- [124] D.C. Wilcox (3rd ed.), *Turbulence Modelling for CFD*, 2006 DCW Industries.
- [125] <https://www.afs.enea.it/project/neptunius/docs/fluent/html/th/node66.htm>, accessed: 10.07.2022
- [126] D.K. Rajak, P.L. Menezes, *Application of Metal Matrix Composites in Engineering Sectors*, 2021 Elsevier Ltd.
- [127] E.A.M. Shalaby, A.Y. Churyumov, *Journal of Alloys and Compounds*, Development and characterization of A359/AlN composites for automotive applications **727**, 540-548 (2017).  
DOI: <https://doi.org/10.1016/j.jallcom.2017.08.154>
- [128] S. Senthil, M. Raguraman, D.T. Manalan, *Materials Today: Proceedings*, Manufacturing processes & recent applications of aluminium metal matrix composite materials: A review **45**, 5934-5938 (2020).  
DOI: <https://doi.org/10.1016/j.matpr.2020.08.792>
- [129] V.M. Kumar, C.V. Venkatesh, *Materials Research Express*, A comprehensive review on material selection, processing, characterization and applications of aluminium metal matrix composites **6**, 7 (2019).  
DOI: <https://doi.org/10.1088/2053-1591/ab0ee3>
- [130] F. Nturanabo, L. Masu, J.B. Kirabira, *Novel Applications of Aluminium Metal Matrix Composites*, in: K. Cooke, *Aluminium Alloys and Composites 2020*, IntechOpen 2020.  
DOI: <https://doi.org/10.5772/intechopen.86225>
- [131] <https://ceramics.ferrotec.com/materials/metal-matrix/al-sic/>, accessed: 06.12.2022
- [132] <https://www.ceramtec.in/ceramic-materials/metal-matrix-composites/>, accessed: 06.12.2022
- [133] <https://ii-vi.com/product/metal-matrix-composites/>, accessed: 06.12.2022